(2)

ONR-URI Composites Program
Technical Report No. 11

UIUC-NCCMR-89-#0011

THERMAL CURING CYCLES FOR COMPOSITE CYLINDERS WITH THICK WALLS AND THERMOSET RESINS*

L. N. Hjellming** and J. S. Walker***

June 1, 1989

National Center for Composite Material Research
at University of Illinois, Urbana - Champaign
A DoD University Research Initiatives Center funded by the
Office of Naval Research, Arlington, VA

---

* submitted to Journal of Composite Materials

** Graduate Research Assistant, Department of Theoretical and Applied Mechanics. Current address: Department of Mechanical Engineering and Engineering Science, University of North Carolina at Charlotte, Charlotte, NC 28223

*** Professor, Department of Mechanical Engineering

Motion of Continuous Fibers through a Newtonian Resin for High Fiber Volume Fraction

L.N. Hjellming*
Department of Mechanical Engineering and
Engineering Science
University of North Carolina at Charlotte
Charlotte, NC 28223
and
J.S. Walker
National Center for Composite Materials Research
University of Illinois
Urbana, IL 61801

ABSTRACT

This paper treats the motion of long, unidirectional, continuous fibers through a Newtonian resin. There is a consolidation force on the top row of fibers or an effective force on all the fibers due to their tension in a filament-wound cylinder. An asymptotic analysis for high fiber volume fraction is presented here. The results of the present rigorous asymptotic solution are compared to the results of a previous application of the lubrication approximation.

*Author to whom correspondence should be addressed.

1. INTRODUCTION

There are several objectives to be achieved during the consolidation of a composite material. The elimination of voids, the removal of air and excess resin, a uniform degree of cure, a uniform final fiber volume and conformation to a specified fiber orientation are all necessary in the final consolidated material. The consolidation process may be initiated with a surface or pressure loading, or in the case of fiber winding, consolidation results from the fiber tension due to the winding. Both types of loading produce resin and void motion, and this motion depends on the resin matrix properties (such as viscosity, thermal conductivity, cure behavior), the initial fiber volume fraction, fiber orientation, and fiber properties (thermal conductivity, diameter, fiber length).

The work presented here is concerned with the resin flow and fiber motion in a fiber-resin system with an initially high fiber volume typical of composites made with thermoplastic resins. We use an approximate approach to the analysis of the resin flow which (1) will reveal much of the important physical phenomena associated with the non-Newtonian resins, (2) will provide reasonably good quantitative predictions, and (3) will indicate key simplifications to the full boundary value problems which can then make a more accurate model tractable.

The approximate approach represents an extension of a model

developed by Lindt [1] for fiber motion in a Newtonian resin. Lindt assumes a rectangular array of fibers arranged in parallel rows and constrained to vertical motion only. Lindt assumes that the important resin flows are in the gaps between the fiber rows and columns, and uses lubrication theory to treat these flows. A correct version of this model represents the leading order term in an asymptotic solution for $\varepsilon \ll 1$, where ε^2 is the ratio of the gap size to the fiber radius. The model is not restricted to Newtonian fluids; the only restriction is for the fiber volume to be large, corresponding to narrow gaps between fibers. As thermoplastic prepreg tape for filament winding has little or no excess resin, this asymptotic solution will be reasonably accurate for thermoplastic resin flows.

We begin by presenting the asymptotic solution for a Newtonian fluid in order to compare our results with the results of Lindt. This will provide a check on this work and on Lindt's work. The solution presented here is a rigorous asymptotic solution for $\varepsilon \ll 1$, with matching between the subregions in each narrow gap. In a future paper, the model will be applied to non-Newtonian fluids and irregular fiber arrays. In section 2 the flow field in the narrow gap regions will be determined, with the forces on the fibers due to these flows derived in section 3. The numerical analysis and consolidation results are presented in section 4.

2. PROBLEM FORMULATION FOR NEWTONIAN RESIN FLOW

We consider the resin and fiber motion in a system of n rows of moving fibers suspended in a high viscosity Newtonian fluid. The fiber length is much larger than the fiber radius, and the flow along the fiber length is negligible. The fibers are arranged in columns, with the separation between adjacent columns equal to $2b_0$. The adjacent fiber rows are separated by a distance $2h_i(t)$, where i denotes the row of the fiber above, and the row gap is a function of time. The fiber columns are constrained to remain in columns with the same gap size for all time t. The geometry of the fiber-resin system is shown in figure 1. All fibers are subjected to an applied force due to the fiber tension and the top row of fibers is subjected to a distributed surface force per unit length due to the consolidation process.

The Reynold's number for the resin is $Re=\rho U_c R/\mu$, where ρ and μ are the density and viscosity of the resin, while U_c and R are the characteristic velocity and fiber radius. For consolidation with polymeric fluids, $Re \ll 1$, so that the inertial "force" associated with the resin acceleration is negligible compared to the viscous force between the fiber and resin. Since the density of the fibers is comparable to that of the resin, the inertial "force" associated with the fiber acceleration is also negligible. Therefore, there is an equilibrium of the vertical forces for each fiber.

There are two flow regimes for the given geometry. The flow between adjacent rows, caused by the applied loading of the fibers and subsequent vertical motion of the fiber rows, is called the **squeezing flow**, after Lindt [1]. This flow is the source of fluid which flows through the gaps between the adjacent columns, which is called the **normal flow**, again after Lindt [1].

A. Squeeze Flow Between Fiber Rows

For the squeeze flow between fiber rows, the top fiber (in row i) moves downward with a velocity $V_i(t)$ and the bottom fiber (in row i+1) moves downward with a velocity $V_{i+1}(t)$. We choose a coordinate system with an origin which is aligned with the fiber centers and remains midway between the fiber row gap, as shown in figure 2(a). Thus the origin moves with a velocity $U_i = -(V_i+V_{i+1})/2$ relative to a fixed coordinate frame. In the moving frame, the top fiber i moves downward with a velocity

$$-\eta_i = -\left|\frac{V_i - V_{i+1}}{2}\right| \tag{1a}$$

while the bottom fiber i+1 moves upward with a velocity

$$\eta_i = \left|\frac{V_i - V_{i+1}}{2}\right| \tag{1b}$$

The squeezing flow between the i and i+1 fibers is symmetric about the x=0 and y=0 planes. The position of the top fiber surface is given by

$$R^2 = x^2 + (y-R-h_i)^2 \tag{2}$$

This can be rewritten as

$$y = h_i + R - R(1 - x^2/R^2)^{1/2} \tag{3}$$

where R is the fiber radius and h_i is half the gap size between the i and i+1 rows. Equation (3) can be expanded for $x \ll R$ to give

$$\frac{y}{h_i} = 1 + \frac{x^2}{2Rh_i^2} + O\left[\frac{x^4}{R^3 h_i}\right] \tag{4}$$

The equations governing the inertialess fluid flow are

$$0 = -\nabla p + \mu \nabla^2 \mathbf{u} \tag{5a-c}$$

$$0 = \nabla \cdot \mathbf{u} \tag{6}$$

where $\nabla^2 = \frac{\partial^2}{\partial x^2} + \frac{\partial^2}{\partial y^2}$

and $\mathbf{u}, p, \mu$ are the velocity, pressure and viscosity of the fluid.

We consider first the near region of the squeeze region, where x is comparable to h_1 and both x and h_i are much less than R. For x comparable to h_1, the fiber surface is asymptotically flat, and the surface is at $y/h_1 = 1$. We use the following scalings for region 1

$$y_1 = h_1 y_1^* \quad , \quad x_1 = h_1 x_1^* \tag{7a,b}$$

$$u_y = \eta_1 u_{y_1}^* \quad , \quad u_x = \eta_1 u_{x_1}^* \tag{8a,b}$$

$$p_1 = \frac{\mu \eta_1}{h_1} p_1^* \quad , \quad t = \frac{h_1}{\eta_1} t^* \tag{9a,b}$$

where the dimensionless variables are denoted by an asterisk.

The non-dimensional equations for region 1, with the

asterisks dropped, are

$$0 = -\frac{\partial p_1}{\partial x_1} + \nabla^2 u_{x_1} \tag{10a}$$

$$0 = -\frac{\partial p_1}{\partial y_1} + \nabla^2 u_{y_1} \tag{10b}$$

$$\underset{\sim}{\nabla}\cdot\underset{\sim}{u} = 0 \tag{11}$$

where $\nabla^2 = \frac{\partial^2}{\partial x_1^2} + \frac{\partial^2}{\partial y_1^2}$

Due to the symmetry of the flow and geometry, only the top fiber row i need be considered in determining the squeeze flow. The boundary conditions are

$$u_{y_1} = -1 \quad , \quad u_{x_1} = 0 \qquad \text{at } y_1 = 1 \tag{12a,b}$$

$$u_{y_1} = 0 \quad , \quad \frac{\partial u_{x_1}}{\partial y_1} = 0 \qquad \text{at } y_1 = 0 \tag{13a,b}$$

$$u_{x_1} = 0 \quad , \quad \frac{\partial u_{y_1}}{\partial x_1} = 0 \qquad \text{at } x_1 = 0, \quad 0 \le y_1 \le 1 \tag{14a,b}$$

The boundary conditions (13,14) are symmetry conditions on the squeeze flow and shear stress.

We replace each dependent variable by a Taylor series with powers of x_1 times coefficent functions of y_1. The coefficents for the different powers of x_1 decouple and are governed by ordinary differential equations in y_1. One decoupled problem has an inhomogeneous boundary condition (12a) and thus has a non-zero solution, while all other decoupled problems have homogeneous boundary conditions, and thus have only zero as a solution.

Therefore, the solution represents a Taylor series in x_1 with only one term so that it applies at all x_1. The only non-zero parts of the Taylor series are

$$u_{x_1} = x_1 U_x(y_1) \tag{15a}$$

$$u_{y_1} = V(y_1) \tag{15b}$$

$$p_1 = Ax_1^2 + P(y_1) \tag{15c}$$

When the solutions (15) are substituted into (10,11) and the boundary conditions (12-14) are satisfied, the solutions for region 1 are

$$u_{x_1} = \frac{3}{2} x_1 \left(1-y_1^2\right) \tag{16a}$$

$$u_{y_1} = -\frac{3}{2} y_1 \left(1-\frac{y_1^2}{3}\right) \tag{16b}$$

$$p_1 = -\frac{3}{2}\left(x_1^2 - y_1^2\right) + B \tag{16c}$$

where B is a constant ambient pressure to be determined.

When $x \gg h_i$, the curvature of the surface becomes important. From equation (4), the leading order curvature term is O(1) when x is comparable to $(Rh_i)^{1/2}$. The position of the surface is parabolic in x for region 2 where $h_i \ll x = O(Rh_i)^{1/2} \ll R$, with

$$\frac{y}{h_i} = 1 + \frac{x^2}{2Rh_i} \tag{17}$$

The appropriate scalings for the region 2 flow variables are

$$y_2 = h_1 y_2^* \quad , \quad x_2 = (Rh_1)^{1/2} x_2^* = \frac{h_1}{\varepsilon_1} x_2^* \qquad (18a,b)$$

$$u_{y_2} = \eta_1 u_{y_2}^* \quad , \quad u_{x_2} = \frac{\eta_1}{\varepsilon_1} u_{x_2}^* \qquad (19a,b)$$

$$p_2 = \frac{\mu \eta_1}{\varepsilon_1^2 h_1} p_2^* \qquad t = \frac{h_1}{\eta_1} t^* \qquad (20a,b)$$

where $\varepsilon_1 = (h_1/R)^{1/2}$. Thus for region 2, the x variable is compressed by the factor ε_1 relative to y, which determines the scaling for u_{x_2} from conservation of mass. The rescaled non-dimensional equations, using the scalings (18-20) in equations (5,6), are

$$0 = -\frac{\partial p_2}{\partial x_2} + \frac{\partial^2 u_{x_2}}{\partial y_2^2} \qquad (21a)$$

$$0 = -\frac{\partial p_2}{\partial y_2} \qquad (21b)$$

$$0 = \frac{\partial u_{x_2}}{\partial x_2} + \frac{\partial u_{y_2}}{\partial y_2} \qquad (22)$$

where the asterisks have been dropped, and the $O(\varepsilon_1)^2$ terms have been neglected. The boundary conditions are

$$u_{y_2} = -1 \quad , \quad u_{x_2} = 0 \qquad \text{at } y_2 = f_2(x_2) = 1 + \frac{x_2^2}{2} \qquad (23a,b)$$

$$u_{y_2} = 0 \quad , \quad \frac{\partial u_{x_2}}{\partial y_2} = 0 \qquad \text{at } y_2 = 0 \qquad (24a,b)$$

$$u_{y_2} \to u_{y_1} \quad , \quad u_{x_2} \to u_{x_1} \qquad \text{as } x_2 \to 0 \qquad (25a,b)$$

Condition (25) is a matching condition between region 2 and region 1.

Solving (21,22) with the boundary conditions (23-25) yields the solutions

$$u_{x_2} = -\frac{dp_2}{dx_2}\left(f_2^2 - y_2^2 \right) \tag{26a}$$

$$u_{y_2} = \frac{1}{2}\frac{d^2p_2}{dx_2^2}\left\{ y_2 f_2^2 - \frac{y_2^3}{3} \right\} + x_2 y_2 f_2^2 \frac{dp_2}{dx_2} \tag{26b}$$

$$p_2 = \frac{\Sigma}{2f_2^2} \tag{26c}$$

where p_2 represents the dimensionless elevation of the pressure in the squeeze gap above the ambient pressure for $x_2 \gg 1$. The pressure is an even function of x_2. The solutions (26) with $x_2 = \varepsilon x_1 \ll 1$ match the inner region 1 solutions (16) with $x_1 = x_2/\varepsilon \gg 1$, and this matching determines B=1 in the inner region 1 pressure (16c).

The fluid squeezed out between the i and i+1 fibers is the source of fluid flow through the gaps between the fiber columns. It is this normal flow which is considered next.

B. Normal Flow between Fiber Columns

As shown in figure 2(b), the adjacent fiber columns are separated by a distance $2b_o$, where b_o remains constant throughout the consolidation process. The fibers in row i move with a velocity V_i. For the normal flow, we use a coordinate system at rest with fiber row i, with the origin of the coordinate system midway between the adjacent columns. The surface of the fiber is

given by

$$(x-\delta_o-R)^2 + y^2 = R^2 \tag{27a}$$

or

$$x = \delta_o + R \pm (R^2 - y^2)^{1/2} \tag{27b}$$

In the normal gap, there is no interior region analagous to region 1 of the squeeze flow. The appropriate scalings for the equations (5,6) in the normal gap are

$$x = \delta_o x^* \quad , \quad y = \frac{\delta_o}{\varepsilon_n} y^* \quad , \quad \varepsilon_n = \left[\frac{\delta_o}{R}\right]^{1/2} \tag{28a,b,c}$$

$$u_{x_n} = V_1 u^*_{x_n} \quad , \quad u_{y_n} = \frac{V_1}{\varepsilon_n} u^*_{y_n} \tag{29a,b}$$

$$p_n = \frac{\mu V_1}{\varepsilon_n^2 \delta_o} p^*_n \quad , \quad t = \frac{\delta_o}{V_1} t^* \tag{30a,b}$$

For the normal gap region $\delta_o << y = O(R\delta_o)^{1/2} << R$, the non-dimensional equations governing the fluid flow in the ith normal gap region are

$$0 = -\frac{\partial p_n}{\partial x} \tag{31a}$$

$$0 = -\frac{\partial p_n}{\partial y} + \frac{\partial^2 u_{y_n}}{\partial x^2} \tag{31b}$$

$$0 = \frac{\partial u_{x_n}}{\partial x} + \frac{\partial u_{y_n}}{\partial y} \tag{31c}$$

where the asterisks have been dropped, and $O(\varepsilon_n^2)$ terms have been

neglected. Because of the symmetry of the flow, only one side of the ith fiber column need be considered. Here, we treat the right side of the column cell. The boundary conditions on the normal flow at the fiber surface are

$$u_{x_n} = 0 \quad , \quad u_{y_n} = 0 \qquad \text{at } x = f_n(y) = 1 + \frac{y^2}{2} \qquad (33a,b)$$

in a frame of reference at rest with the fiber row i. The position of the surface is found by an expansion of (27b) using the scalings (28). The symmetry condition is given by

$$\frac{\partial u_{y_n}}{\partial x} = 0 \quad , \quad u_{x_n} = 0 \qquad \text{at } x=0 \qquad (34a,b)$$

so that u_{y_n} reaches an extremum at the center of the normal gap.

There is an additional condition on the normal flow which represents a constraint on the amount of fluid passing through the ith column gaps. The fluid which is squeezed out of the region between the i and i+1 fiber rows is forced into the i column gaps, and hence flows upward. In the region between the i+1 and i+2 rows, fluid is also lost due to squeezing and is forced into the i+1 column gaps and upwards through the i normal gaps, the i-1 normal gaps, and so on until the fluid reaches the top fiber row. The total volume occupied by the resin-fiber columns changes as the fluid is removed from the squeeze region, while the size of the column gaps remain constant. The change in volume of the column from row i to row n (the static bottom fiber row) in a time Δt is

equal to the volume of fluid which is squeezed and then passes through the column gaps. Thus Q_i, the volume flow rate per unit length passing through the ith column gap, is given by

$$Q_i = 2\left[R + \delta_o\right]\frac{V_i \Delta t}{\Delta t}$$

where $2(R+\delta_o)$ is the horizontal size of the column cell about fiber 1 and $V_i \Delta t$ is the total change in the vertical size of the 1 to n column cells. Then Q_i represents the accumulated flow due to the squeezing between the fiber rows from i to n. The above expression for Q_i can be simplified and rewritten as

$$Q_i = 2\left[R + \delta_o\right]V_i \tag{35}$$

It should be noted that the total volume flow rate per unit length can be calculated from the top fiber row velocity with i=1; this determines the net loss of resin in the system.

The volume flow rate per unit length Q_i corresponds to the flux of fluid through the ith column gap. Thus, using the scalings (28-30), the conservation of mass condition is

$$2\int_0^{f_n(y)} u_{y_n}\, dx = \frac{Q_1 \varepsilon_n}{V_1 \delta_o} \tag{36}$$

For simplicity, we use the notation

$$q_i = \frac{Q_i \epsilon_n}{2V_i \delta_o} = \epsilon_n + \frac{1}{\epsilon_n} \tag{37}$$

Equations (31,32) are solved, using the boundary conditions (33,34) and conservation of mass (36), for the normal gap flow. The solutions are

$$u_{x_n} = \frac{1}{2} \frac{d^2 p_n}{dy^2} \left\{ f_n^2 x - \frac{x^3}{3} \right\} + xy f_n \frac{dp_n}{dy} \tag{38a}$$

$$u_{y_n} = -\frac{1}{2} \frac{dp_n}{dy} \left\{ f_n^2 - x^2 \right\} \tag{38b}$$

$$\frac{dp_n}{dy} = -\frac{3q_i}{f_n^3} \tag{38c}$$

From equation (38c) it is seen that there is a pressure drop across the normal gap which drives the flow upward toward the surface of the system, and that this pressure depends on the volume flow rate. As $y \to 0$, the solution (38) becomes simple Poiseuille flow between parallel walls at $x = \pm 1$, which is the correct solution for the normal flow when the dimensional x and y are both comparable to δ_o. While the squeezing flow requires a special solution in the interior region 1, the normal flow does not require an inner region, as previously stated.

3. FORCE BALANCE ON THE FIBERS

Since the inertial "force" due to the fiber accelerations is

negligible compared to the viscous forces of the resin on the fiber, the sum of the forces on the fibers must be zero. The forces on the fiber have two sources: (1) the externally applied force due to a fiber tension or distributed surface force per unit length, and (2) the force the fluid exerts on the fibers. The externally applied force per unit length is denoted as

$$\underset{\sim}{F}^{i}_{ext} = -T_i \hat{y} \tag{39}$$

where the applied load acts in the $-\hat{y}$ direction with a magnitude of T_i at each fiber row.

The forces the fluid exerts on the ith fiber surface are found using the relation

$$dF^{i}_{j} = \sigma^{i}_{jk} n_k dA \tag{40}$$

where σ^{i}_{jk} is the stress tensor for the fluid due to flow about the ith fiber. Equation (40) is the incremental force in the jth direction which acts on an incremental surface area element dA which has a unit vector n_k.

A. Force due to the squeezing flows

There are two parts to the force on the ith fiber row due to the squeezing flows. The first part is the force on the ith fiber due to the squeeze flow between the i and i+1 fiber rows acting on the bottom of the ith fiber. The second part of the

force is due to the squeeze flow between the i-1 and i fiber rows, acting at the top of the ith fiber.

The first step to finding the forces due to the squeezing flow is to find the normal vector. The normal vector to a surface is given by

$$\hat{n} = \frac{\nabla G}{|\nabla G|} \tag{41}$$

where G=0 is the equation of the surface. Using equation (3), the surface equation for the squeeze flow cell is given by

$$G = R + h_i - y - (R^2 - x^2)^{1/2} = 0 \tag{42}$$

The normal vector to the top surface in the ith squeeze region is

$$\hat{n} = \frac{x}{R}\hat{x} - \frac{(R^2-x^2)^{1/2}}{R}\hat{y} \tag{43a}$$

where $\hat{x}$ and $\hat{y}$ are unit vectors. By substituting the scalings (18) into the expression (43a) , the normal vector becomes

$$\hat{n} = \varepsilon_1 x_2^* \hat{x} - \hat{y} \tag{43b}$$

where the $O(\varepsilon_1)^2$ terms have been neglected in order to remain consistent with previous approximations. The area element dA for the surface is found by a similar analysis. For a circular surface

$$dA = R d\theta \ , \quad \text{where } \theta = \tan^{-1}\left|\frac{x_2}{-(y_2 - R - h_1)}\right| \tag{44}$$

and $d\theta = \frac{\partial \theta}{\partial x_2} dx_2 + \frac{\partial \theta}{\partial y_2} dy_2$

Ignoring $O(\varepsilon_i)^2$ terms, the area element (44) is given by

$$dA = dx_2 \tag{45}$$

Thus, with (40,43b,45), the forces on the ith fiber row due to the squeezing flow are

$$F^i_{x_{sq}} = \int_{-\infty}^{+\infty} \left(\varepsilon_i x_2^* \sigma_{xx} - \sigma_{xy} \right) dx_2 \tag{46a}$$

$$F^i_{y_{sq}} = \int_{-\infty}^{+\infty} \left(\varepsilon_i x_2^* \sigma_{yx} - \sigma_{yy} \right) dx_2 \tag{46b}$$

where the limits are the asymptotic limits of the surface, and the asterisks denote the non-dimensional variables.

For an incompressible, Newtonian fluid the stress is given by

$$\sigma_{jk} = -p\delta_{jk} + \mu \left(\frac{\partial u_j}{\partial x_k} + \frac{\partial u_k}{\partial x_j} \right) \tag{47}$$

The scalings (18,19,20a) and the squeeze flow solutions (26) are substituted into (47). The integrand in (46a) is an odd function of x and thus gives a zero net contribution to the $\hat{x}$ force (46a). This is seen by examining the solutions (26): the pressure is an even function in x_2 as is the normal stress $(\partial u_{x_2} / \partial x_2)$, while the shear stress $(\partial u_{x_2} / \partial y_2)$ is odd in x_2.

There is a force in the $\hat{y}$-direction due to the pressure. With the pressure given by equation (26c), equation (46b) becomes

$$F^{i}_{y_{sq,bot}} = \frac{\mu n_i}{\varepsilon_i^3} \int_{-\infty}^{+\infty} p_2^* dx_2^* = \frac{3\pi\mu n_i}{2\sqrt{2}\ \varepsilon_i^3} \qquad (48a)$$

This gives the force on the bottom of the ith fiber row in the $\hat{y}$-direction due to the pressure generated by the squeezing flow between the i and i+1 fiber rows. The force on the top of the ith fiber row is directed downward, and is given by

$$F^{i}_{y_{sq,top}} = -\frac{3\pi\mu n_{i-1}}{2\sqrt{2}\varepsilon_{i-1}^3} \qquad (48b)$$

This force is due to the squeezing flow between the i-1 and i fiber rows. We have used the pressure (26c) throughout the squeeze gap region, but there is a very small region with $x=O(h_i)$ where the pressure is given by equation (16c) with B=1. The pressure in the region $x=O(h_i)$ is slightly less than the pressure predicted by (26c). However, the deviation is $O(\varepsilon_i)^2$ and extends over a small, $O(\varepsilon_i)$ portion of the surface, so that the error is $O(\varepsilon_i)^3$ smaller than the forces in equations (48).

B. Force due to the normal flow

To calculate the force due to the normal flow, we proceed as we did for the squeezing flow. Using the expression (27b), the equation for the right fiber surface in the normal gap is

$$G = \delta_o + R - (R^2 - y^2)^{1/2} - x = 0 \tag{49}$$

The unit normal vector, found using the equations (28,41,49), is given by

$$\hat{\mathbf{n}} = -\hat{\mathbf{x}} + \varepsilon_n y^* \hat{\mathbf{y}} \tag{50}$$

neglecting $O(\varepsilon_n)^2$ terms, and the asterisks denote the non-dimensional variables. The area element is dA=dy. Using equations (40,50), the forces due to the normal flow at the fiber surface are

$$F^1_{x_n} = \int_{-\infty}^{+\infty} \left[-\sigma_{xx} + \varepsilon_n y^* \sigma_{xy} \right] dy \tag{51a}$$

$$F^1_{y_n} = \int_{-\infty}^{+\infty} \left[-\sigma_{yx} + \varepsilon_n y^* \sigma_{yy} \right] dy \tag{51b}$$

where the limits are the asymptotic limits for the region. The scalings (28-30a) and the solutions (38) for the normal flow are substituted into equations (47,51). The result for the force in the x-direction is

$$F^1_{x_n} = \frac{\mu V_1}{\varepsilon_n^3} \int_{-\infty}^{+\infty} p_n dy \tag{52}$$

where the integrand is in terms of the non-dimensional variables, and the asterisks have now been dropped. By examining the solution

(38c), the integrand of (51a) is shown to be an odd function of y. Thus, the force $F^i_{x_n}$ due to the normal flow is zero.

The force in the $\hat{y}$-direction due to the normal flow is

$$F^i_{y_n} = \frac{\mu V_i}{\varepsilon_n^2} \int_{-\infty}^{+\infty} \left[-yp_n - \frac{\partial u_{y_n}}{\partial x} \right] dy \qquad (53)$$

where the integrand of (53) is in terms of the non-dimensional variables (28-30), and $O(\varepsilon_n)^2$ terms have been neglected. This force (53) is produced by the pressure distribution and shear stress at the fiber surface.

Before evaluating equation (53), the pressure distribution in the normal gap is determined by integrating the equation (38c) to obtain

$$p_n = -q_i \left\{ \frac{3y}{\left[2 + y^2 \right]^2} + \frac{9y}{4\left[2 + y^2 \right]} + \frac{9}{4\sqrt{2}} \tan^{-1}\left[\frac{y}{\sqrt{2}} \right] \right\} \qquad (54)$$

The first two terms in the expression (54) approach zero as $y \to \pm\infty$, but the last term approaches two different constant pressures as $y \to \pm\infty$, so that

$$\Delta p_n = p_n(y \to \infty) - p(y \to -\infty) = -\frac{9\pi q_i}{4\sqrt{2}} \qquad (55)$$

This Δp_n is the pressure drop needed to drive the flow Q_i through the normal gap between the adjacent fibers in the ith row. Therefore, the ambient pressure above the ith fiber is less than the ambient pressure below the ith fiber. The solutions (26,38,54)

give the velocity and pressure in the squeeze and normal gaps, gaps which represent a small, $O(\varepsilon)$ fraction of the total fiber surface. The pressure drop (55) gives a pressure over the entire bottom of the fiber, a pressure which is greater than the pressure over the entire top of the fiber by a value $|\Delta p_n|$. This pressure difference produces a net upward force on the fiber. We cannot obtain this force by introducing the expression (54) into equation (53), as the unit normal vector (50) is valid only in the normal gap region where the fiber locally appears to be a parabola. If we were to introduce the pressure (54) into the force expression (53), we would obtain an infinite force, because there is a pressure difference across a parabolic surface, which has an infinite area.

To find the total vertical force due to the normal flow, we first consider the vertical force due to the change in the dimensional ambient pressure

$$\pm \frac{\Delta p_n \mu V_i}{2\delta_o \varepsilon_n^2}, \qquad \text{for} \quad y \gtrless 0 \tag{56}$$

on the top and the bottom halves, respectively, of the fiber with the true circular cross section. This gives a pressure force per unit fiber length,

$$F^i_{y_p} = \frac{9\pi q_i \mu V_i}{2\sqrt{2}\varepsilon_n^4} \tag{57}$$

Since the force due to the pressures (56) has been accounted for in the pressure force (57), the expression (53) is replaced by the expression

$$F^{1}_{y_n} = -\frac{\mu V_i}{\varepsilon_n^2}\int_{-\infty}^{+\infty}\left\{ y\left|\frac{-\Delta p_n}{2}\,\mathrm{sgn}(y) + p_n\right| + \frac{\partial u_{y_n}}{\partial x}\right\} dy \qquad (58)$$

for the force per unit length on the left side of the ith fiber, due to the local parts of the normal gap flow. The integral (58) with the expressions (38,54,55) is well defined and gives

$$F^{1}_{y_n} = \frac{9\pi\mu V_i q_i}{4\sqrt{2}\varepsilon_n^2} \qquad (59)$$

By symmetry, the force per unit length on the right side of the ith fiber is also given by the expression (59). The total normal force due to the ambient pressure and local parts of the normal flow is given by

$$F^{i}_{y_{n,tot}} = F^{1}_{y_p} + 2F^{1}_{y_n} = \frac{9\pi\mu V_1}{2\sqrt{2}\varepsilon_n^5}\left|\varepsilon_n^2 + 1\right|^2 \qquad (60)$$

As the inertial force associated with the fiber accelerations is negligible, the downward force per unit length (39) must equal the upward forces due to the squeeze and normal flows, where

$$T_i = F^{i}_{y_{sq,bot}} + F^{1}_{y_{sq,top}} + F^{i}_{y_{n,tot}} \qquad (61)$$

Introducing equations (1,37,48,60), the force balance (61) becomes

$$T_i = \frac{3\pi\mu(V_i - V_{i+1})}{4\sqrt{2}\varepsilon_i^3} - \frac{3\pi\mu(V_{i-1} - V_i)}{4\sqrt{2}\varepsilon_{i-1}^3} + \frac{9\pi\mu V_1}{2\sqrt{2}\varepsilon_n^5}\left|1 + \varepsilon_n^2\right|^2 \qquad (62)$$

Equation (62) is the force balance for a system of n-moving fibers with squeeze gaps $2h_1$ which satisfy the condition $h_1 \ll (Rh_1)^{1/2} \ll R$, and normal gaps $2\delta_o$ which satisfy $\delta_o \ll (R\delta_o)^{1/2} \ll R$.

The force balance given in (62) is applicable for all interior fibers, i=2 to n-1. The nth fiber is considered to be stationary; the bottom fiber is constrained by a solid surface and so remains motionless, with the fibers above it moving toward the nth fiber. The top fiber i=1 has no squeezing flow due to a fiber above it. Thus, for i=1, the force balance (62) is modified to

$$T_1 = \frac{3\pi\mu}{4\sqrt{2}\varepsilon_1^3}\left|V_1 - V_2\right| + \frac{9\pi\mu V_1}{2\sqrt{2}\varepsilon_n^5}\left|1 + \varepsilon_n^2\right|^2 \qquad (63)$$

4. NUMERICAL CALCULATIONS AND CONSOLIDATION RESULTS

The consolidation behavior of the set of n-moving fibers is determined by solving the set of n-1 simultaneous equations (62,63), with the condition that the i=n fiber is stationary, for the fiber velocities, fiber displacements and volume flow rate per unit length. To facilitate the calculation, the following scalings are used in (62,63),

$$T_i = T_c T_i^* \quad , \quad t_c = \frac{R\mu}{T_c} \qquad (64a,b)$$

$$V_i = \frac{R}{t_c} V_i^* \quad , \quad h_i = R h_i^* \quad , \quad \delta_o = R \delta_o^* \qquad (64c\text{-}e)$$

$$\varepsilon_i = \left| h_i^* \right|^{1/2} \quad , \quad \varepsilon_n = \left| \delta_o^* \right|^{1/2} \qquad (64f,g)$$

where the asterisks denote the non-dimensional quantites.

The value of T_c is taken to be the magnitude of the tension in the fibers or of the distributed surface force per unit length. The characteristic time is determined using the fluid viscosity, fiber radius and characteristic applied force T_c. Since the characteristic time depends on the fluid viscosity, a change in the viscosity will change the value of t_c, and the characteristic velocity, R/t_c. Similarly, a change in the value of the characteristic applied force will change t_c as well as the characteristic velocity.

With the scalings (64), the force balance equations (62,63) are rewritten as

$$T_1^* = \frac{3\pi}{4\sqrt{2}\varepsilon_1^3} \left| V_1^* - V_2^* \right| + \frac{9\pi \left| \varepsilon_n^2 + 1 \right|^2 V_1^*}{2\sqrt{2}\varepsilon_n^5} \qquad (65)$$

$$T_1^* = \frac{3\pi}{4\sqrt{2}\varepsilon_1^3} \left| V_1^* - V_{1+1}^* \right| - \frac{3\pi}{4\sqrt{2}\varepsilon_{1-1}^3} \left| V_{1-1}^* - V_1^* \right| + \frac{9\pi \left| \varepsilon_n^2 + 1 \right|^2 V_1^*}{2\sqrt{2}\varepsilon_n^5} \qquad (66)$$

As fluid is squeezed out from between the fiber rows, the gap

between the rows will change. To take this into account, the squeeze gap $2h_i$ is updated at each time step, where

$$2h_i(t+\Delta t) = 2h_i(t) + \Delta t(V_{i+1} - V_i)$$

or using the scalings (64)

$$h_i^*(t^* + \Delta t^*) = h_i^*(t^*) + \Delta t^*(V_{i+1}^* - V_i^*)/2 \qquad (67)$$

The equations (65,66), along with the zero velocity condition on the nth fiber, are formed into a set of simultaneous equations of the form $L_{ji}V_i^*=T_j^*$. The fiber velocities are found using a routine for solving sets of simultaneous linear algebraic equations [2]. Once the velocities are known, the squeeze gaps $2h_i^*$, using equation (67), are updated and the next time step is performed until $t^*=t_{max}$.

A. Consolidation from the top: Lindt's problem

We consider first the calculation corresponding to one of Lindt's systems for n=12 fibers. The top fiber row (i=1) is loaded by a distributed surface force per unit length, T_1=0.005N/m, and there are no other applied forces on the interior fibers i=2-12. The fluid viscosity is 10kg/m-s and the fiber radius, R, is taken to be 10^{-5}m. The initial gaps are given by

$$h_i(t^*=0) = \delta_o = R = 10^{-5}m \qquad (68)$$

The characteristic time, t_c, is 0.02 seconds. Half the dimensionless distance between the fiber rows, h_i^*, for (i=1-5) and

the dimensionless fiber velocities, V_i^*, for (i=1-5), are shown in figure 3(a) and 3(b) respectively. The volume flow rate per unit length may be calculated directly from the fiber velocities using (35) and the scalings (64). The dimensional flow rate per unit length is given by

$$Q_i = 10^{-8}(1 + \delta_o^*)V_i^* \quad m^2/s \tag{69}$$

The dimensionless normal force (60) and dimensionless squeeze force (48) for the i=1 fiber is shown in figures 4(a), and figure 4(b) shows the dimensionless normal and squeeze forces for the i=2-4 fibers.

The results for this problem can be intrepreted as a type of 'consolidation wave'. Consider the i=1 fiber for $t \approx 0$, when the velocity of the i=2 fiber is close to zero. From (65), the ratio of the normal force to the squeeze force,

$$\frac{F_{1_n}^*}{F_{1_{sq}}^*} \approx \frac{6\left|\varepsilon_n^2 + 1\right|^2}{\varepsilon_n^5}\varepsilon_1^3 \tag{70}$$

For $\varepsilon_n=1$, initially $\varepsilon_1 \approx 1$, the normal force is 24 times larger than the squeeze force. The i=1 fiber is then in a free fall due to the applied force, with the resistive force due to the normal flow only; the interaction between fiber 1 and fiber 2 due to the squeezing flow is very small. The velocity V_1^* is then controlled by the normal flow, and the velocity can be determined by the

balance between the applied force and the normal force, with $T_1^*=1$

$$1=T_1^* = \frac{9\pi\left[\epsilon_n^2+1\right]^2}{2\sqrt{2}\epsilon_n^5} V_1^* \quad , \tag{71}$$

then $V_i^*=0.025$ for $\epsilon_n=1$. The squeeze force acting on the bottom of the i=1 fiber and top of the i=2 fiber is small, but it does influence the i=2 fiber. As the i=1 fiber moves downward, the squeeze force increases in magnitude, since $F_{sq}\propto\epsilon_1^{-3}$. Thus, the force balance requires that the normal force acting on the i=1 fiber decrease as the squeeze force increases. From equation (60) it is seen that $F_n\propto V_i$, so the velocity of the i=1 fiber must decrease to decrease the normal force. The squeeze force acting on the i=1 and i=2 fibers begins to increase the velocity of the i=2 fiber from zero, in turn increasing the normal force on the i=2 fiber, while the i=2 fiber velocity is less than the i=1 fiber velocity. When the squeeze gap between the i=1 and i=2 fibers becomes small, the squeeze force acting on the i=1 fiber begins to dominate. This occurs at t≈2.4 seconds for the i=1,2 fibers. At this time, the squeeze force acting on the i=2 fiber is mainly due to the interaction between the i=2 and i=1 fibers, with the interaction between the i=2 and i=3 fibers very small, and the i=3 fiber almost stationary.

The applied load T_1^* is distributed between the i=1 and i=2 fibers, after t≈2.4 seconds. The normal force on the two fibers is equal, but only half the value of the initial normal force on the i=1 fiber only. The squeeze force acting on the two fibers is

equal in magnitude but opposite in direction. The two fibers are then carrying the same load, and begin to move downward with the same velocity. This velocity is roughly one-half the free-fall velocity for one fiber, as now the applied load has been split into two. These two fibers have formed a consolidation front.

As the top two fibers move downward, the i=3 fiber begins to be influenced by the decrease in the squeeze gap, $2h_2^*$, between the i=2 and i=3 fibers. The squeeze forces acting on the bottom part of the i=2 fiber and the top part of the i=3 fiber increases in magnitude as the squeeze gap decreases. As yet, the i=4 fiber is stationary and does not contribute to the overall force balance. Since the squeeze force on the i=3 fiber is non-zero, the fiber begins to move, slowly at first, but increasing as the i=2 fiber approaches. The velocity of the i=3 fiber produces a normal flow, and hence a normal force, which opposes the squeeze force acting on the top of the i=3 fiber (with no squeeze force acting on the bottom of the i=3 fiber) and gives a balance of the forces. The total squeeze force acting on the i=2 fiber decreases with the addition of the opposing squeeze force on the bottom of the i=2 fiber. This decreases the velocity of the i=2 fiber further, and through the force interaction, the i=1 velocity is also reduced. Because the i=3 fiber has no interaction with the i=4 fiber as yet, the i=3 fiber velocity steadily increases, although remaining less than the velocities of the i=1,2 fibers.

When the squeeze gap between the i=2 and i=3 fibers becomes

small, the total squeeze force acting on the i=3 and i=2 fibers are equal. This occurs at t≈7 seconds. Further, force balance requires that the normal forces are also equal. The normal force acting on the i=1-3 fibers is one-third of the initial normal force acting on the i=1 fiber. The applied force at t≈7 seconds has then been distributed among the three fibers, forming a three fiber consolidation front, which moves with a velocity which is one-third the free-fall velocity for one fiber.

This consolidation process continues as the consolidation front moves downward toward the fiber directly below the front. Once the squeeze gap becomes sufficently small for the total squeeze force on the bottom fiber in the front to equal the squeeze force acting on the top of the fiber directly below the front, the fiber below becomes a part of the consolidation front. This process simply propagates downward row by row, with a velocity which decreases as each row is added. The front starts to move with a free-fall velocity determined by the balance between the normal force and an applied load distributed among the ℓ-fibers in the front. This front free-fall velocity is

$$V^*_{free} = \left\{ \frac{2\sqrt{2}T^*_1 \varepsilon_n^5}{9\pi\ell\left|\varepsilon_n^2 + 1\right|^2} \right\} \qquad (72)$$

where ℓ is the number of fibers in the consolidation front.

The key to the consolidation is in the normal flow. From (60) it is seen that the normal force is strongly dependent on the

size of the normal gap. For large normal gaps, the fluid from the squeezing flow encounters little resistance as it flows into the normal gap region, and so the consolidation front can propagate rapidly. However, as the normal gap is decreased in size, the resistance term, here defined as

$$W_r = \frac{\left(\epsilon_n^2 + 1\right)^2}{\epsilon_n^5} \tag{73}$$

becomes large, and so the free fall velocity of the front (72) is reduced. This indicates that the fluid in the squeeze region cannot penetrate into the normal gap, and so consolidation is inhibited. Figures 5(a-c) show the behavior of a system with the normal gap reduced by half, where δ_o=0.5R. This case has the same loading, viscosity, fiber radius and characteristic time and initial squeeze gap (h(t=0)=R) as the previous case, and the fiber behavior conforms more closely to the free fall analysis already discussed. This is due to the increase in the initial normal force caused by the decrease in the normal gap, where the ratio of the normal force to the squeeze force (70) is increased by about a factor of 3.2. The i=1 fiber is in free fall, with a velocity roughly one-third of the case for δ_o=R; this decrease is directly related to the increase in the normal gap resistance to the flow from the squeezing action between fiber rows 1 and 2. Since the velocities are reduced, the time required for the i=1 fiber to close the squeeze gap sufficently for the squeeze force to dominate

increases. Once the i=1,2 fibers form the front (at t≈7 seconds) the front's velocity is half of the initial free fall velocity, as determined by (72) with ℓ=2. Again, the fibers are moving slowly in a free fall, until the next squeeze gap is small. The value of the size of the squeeze gap at which the normal and squeeze forces are equal, is also reduced as the normal gap size is reduced, as indicated in (70).

If the normal gap is reduced more, the behavior of the consolidation would be similar to the first two cases, but with an increase in the time for the fibers to consolidate, and a stronger conformation to the free-fall behavior previously described.

B. Consolidation with uniform fiber tension

The next case considered is one in which the n-1 fibers have a uniform tension applied. The fiber radius has a value of $R=10^{-5}m$, with $h_1(t=0)=\delta_o=R$, fluid viscosity is 10kg/m-s and the applied force due to the tension of winding on a curve is 0.005N/m, such that $T_i^*=1$ for i=1 to n-1. Half the dimensionless distance between fiber rows, h_i^*, and the dimensionless fiber velocities, V_i^*, are shown in figures 6(a) and 6(b) respectively, with the dimensionless normal and squeeze forces shown in figure 6(c).

The consolidation under uniform fiber tension is similar to the consolidation for uniform top loading. However, with a uniform tension on all of the fiber rows, the consolidation starts at the i=11 fiber and progresses upward. Initially, all n-1 fibers are in

a uniform free-fall (i=n fiber is static), with a free-fall velocity determined by (71) with T_i^* replacing T_1^*. It is the i=11 fiber which experiences a squeezing force due to the presence of the static i=12 fiber. The squeeze force acts on the bottom of the i=11 fiber, with the squeezing force between the i=10 and i=11 fibers initially zero and remaining small. As shown in figure 6(c), the behavior of the normal and squeeze forces for the i=11 fiber is analagous to the force behavior of the i=1 fiber in the uniform top loading case. As the i=11 fiber moves downward toward the static i=12 fiber, the squeeze force increases as the squeeze gap decreases. This necessitates the decrease of the i=11 fiber velocity, to decrease the normal force and maintain the force balance. However, unlike the top loading case, as the i=11 fiber approaches the i=12 fiber, the squeeze force acting on the i=12 fiber does not produce the associated motion of the i=12 fiber, due to the boundary condition that the i=12 or i=n fiber remain static. Thus, the gap between the i=11 and i=12 fibers continues to decrease, with the only resistance to the motion produced by the increasing upward directed squeeze force on the bottom of the i=11 fiber. The ratio of the normal force to the squeeze force for the i=11 fiber under uniform tension is the same as that given in equation (70), with i=1 replaced by i=11. When the squeeze gap, $2h_{11}^*$, is .24 (at t≈1.6 seconds), the normal and squeeze forces acting on the i=11 fiber are equal. As the squeeze gap continues to decrease, the normal force decreases, while the squeeze force

increases and the squeeze gap asymptotically approaches zero extent, with a velocity which also tends to zero. The normal force approaches zero, and the large pressure in the squeeze gap between the i=11 and i=12 fibers produces a sufficent force to balance the uniform tension. The i=11 and i=12 fibers form the consolidation front.

The other fibers are completely unaffected by the interaction between the i=11 and i=12 fibers, and the i=1-10 fibers continue to move in a free-fall with the velocity given by (71). However, once the i=11 fiber has virtually stopped, the i=10 fiber closes the squeeze gap with the now static i=11 and i=12 fibers. The decrease in the squeeze gap between the i=10 and i=11 fiber increases the squeeze force from zero, and this force acts on the bottom of the i=10 fiber. Once the squeeze force on the i=10 fiber begins to increase, the normal force must decrease and the velocity of the i=10 fiber decreases from the free-fall velocity. Once the squeeze gap reaches a value of 0.24 (at t≈3.2 seconds), the squeeze force and normal force acting on the i=10 fiber are equal. Since the i=11,12 consolidation fibers are static, the interaction of the i=10 fiber and the front does not produce any additional motion of the front. Thus, the squeeze gap between the i=10 fiber and the front continues to decrease, until the i=10 fiber reaches the consolidation front. The i=10-12 fibers form the new static consolidation front, and the i=9 fiber moves toward it. This process continues until all 12 or n fibers are stacked.

When the normal gap is reduced, the free-fall velocity of the fibers is decreased according to equation (71). This reduction again arises from the increased resistance of the normal gap to flow through the more narrow channel. The consolidation is much slower, and the size of the squeeze gap for which the squeeze force and normal force are equal is decreased. From equation (70), with δ_o=0.5R, the value of the "critical squeeze gap" is reduced to .11, and the free-fall velocity is reduced by a factor of 3.2. Half the dimensionless distance between fiber rows, the dimensionless velocities and the dimensionless forces for δ_o=0.5R are shown in figure 7(a-c). The fiber velocities are approaching step functions, indicating that the squeeze force remains small for a longer period of time, and that the size of the squeeze gap only contributes to the force when the gap is extremely small. As the normal gap is reduce further, the normal force will remain dominant, due to the large resistance to the normal flow. Only when the squeeze gap approaches zero will the squeeze force rapidly increase and slow the fiber from the free-fall velocity.

5. CONCLUSIONS AND DISCUSSION

This paper treats the vertical motion of long fibers through a Newtonian resin. The horizontal distance, $2\delta_o$, between adjacent fiber columns remains fixed, while the vertical distance, $2h_i(t)$, between the adjacent fiber rows i and i+1 decreases with time. The fiber motion is driven by: (1) a force on the top fiber row due to

an external consolidation force, or (2) a force on each fiber due to its tension and the curvature in a filament-wound cylinder, or (3) any combination of these two forces. Lindt [1] treats the first case with only a force on the top fiber row. Lindt simplifies the two-dimensional inertialess fluid motion equations "using a modified lubrication approximation". We present a rigorous asymptotic solution for $\varepsilon_n=(\delta_o/R)^{1/2}\ll 1$ and $\varepsilon_1=(h_1/R)^{1/2}\ll 1$, where R is the fiber radius. Unfortunately, Lindt does not present any formulae for the fiber velocities, pressures or forces, so that we cannot determine the difference between his lubrication approximation and our asymptotic analysis.

While our analysis is only valid for $\varepsilon_n\ll 1$ and $\varepsilon_i\ll 1$, we present results for $\varepsilon_i=1$ at t=0 and $\varepsilon_n=1$ in order to compare our results in figures 3 and 4 to the results presented by Lindt [1] in his figures 8-10, for the same values of $h_i(t=0)$, δ_o, R, T_1 and μ. At t=0, Lindt predicts a top layer velocity in excess of 1mm/s, while our result in figure 3(b) translates to a dimensional initial top layer velocity which is two orders of magnitude smaller. We suspect that there is an error in the scale for Lindt's figure 8, as a top layer velocity of 1mm/s would consolidate the top two rows in 0.02 seconds, while Lindt indicates that this consolidation takes more than 10 seconds. A more fundamental difference concerns the period of time for adjacent fiber rows to reach equal velocities. Lindt predicts that the top two rows reach an equal velocity at roughly 7 seconds, and that the incremental period for

subsequent rows to reach equal velocities decreases with time. The results in our figure 3(b) indicate that the top two fiber rows reach equal velocities at t=2.4 seconds, and that the period for subsequent row consolidation increases with time, with the increase proportional to the number of fiber rows consolidated. Clearly there are some significant difference between the lubrication solution of Lindt [1] and the present rigorous asymptotic solution for $\varepsilon_n \ll 1$ and $\varepsilon_i \ll 1$. In addition to yielding the correct first order solution for high fiber volume fractions, the asymptotic analysis defines the magnitudes of the neglected terms.

The results for a force on all of the fibers show that the consolidation begins at the bottom fiber row, with the outer fiber rows moving toward the compacted fibers in the interior. We have used only eleven moving fiber rows. However, even this small number is not necessary, since the development of distinct wave fronts would permit a much simplier treatment. The wave fronts are more abrupt for $\varepsilon_n=(0.5)^{1/2}$ than for $\varepsilon_n=1$. As ε_n and ε_i decrease, the normal flows between the fiber columns becomes progressively more dominant. Thus, the squeeze flows provide negligible or constant forces except during the brief periods when a moving fiber comes very close to a static fiber.

The results presented here and by Lindt [1] provide physical insights into the local characteristics of the flows during consolidation. However, for a Newtonian resin, the macroscopic characteristics of consolidation can be derived from Darcy's law

for flow through a porous medium, with local corrections of the permeability as the local fiber volume fraction increases [3]. The more important value of the present model is its potential for treating fiber-resin motions with strongly non-Newtonian resins such as thermoplastics. Darcy's law is restricted to Newtonian fluids. The decoupling of the normal and squeeze flows will provide a significant simplification for a non-Newtonian resin. The purpose of the present paper is to provide a rigorous asymptotic derivation for Lindt's lubrication solution. The accurate definitions of relative magnitudes will be even more important for a non-Newtonian fluid, as the model with a non-Newtonian fluid will involve additional dimensionless parameters, time scales, etc. In a future paper, we will present extensions of the present analysis to some non-Newtonian constitutive equations for thermoset and thermoplastic resins.

ACKNOWLEDGMENT

This research was supported by the Office of Naval Research under contract N800014-86-K-0799, and by a Nation Science Foundation Presidential Young Investigators Award MSS-8957129.

REFERENCES

[1] Lindt, J.T., SAMPE Quarterly, Oct.,pp.14-19, (1982).

[2] Press, W.H.,et. al, Numerical Recipes, Cambridge, UK, Cambridge University Press, (1986).

[3] Dave, R., Kardos, J.L., and Dudukovic, M.P., Polymer Composites, 2:123-132, April (1987).

FIGURE CAPTIONS

FIG. 1 The geometry of the fiber-resin system, with the normal and the squeeze flow regions.

Fig. 2 Close-up of the flow regions. (a) the squeeze flow region with adjacent fiber rows moving with velocities V_i (top row) and V_{i+1} (bottom row. The rows are separated by a distance $2h_1(t)$, and the fiber surface is $y_2=f_2(x_2)$. (b) The normal flow region between adjacent columns separated by a constant gap size 2δ. The fiber surface is at $x=f_n(y)$, and Q_1 indicates the volume flux per unit length through the ith normal gap.

Fig. 3 Results for the Lindt's problem of uniform top loading of the i=1 fiber row only. The force per unit lenth is $T_c=0.005$ N/m, $\mu=10$kg/m-s, fiber radius $R=10^{-5}$m, and $h_1(t=0)=\delta_o=R$. (a) A plot of half the dimensionless distance between adjacent fiber rows, h_i^*, versus time. Shown are the displacements for i=1 to 5. (b) A plot of the dimensionless fiber velocities, V_i^*, versus time, for i=1 to 5. Note the continually decreasing free fall velocity.

Fig. 4 Force results for Lindt's problem of uniform top loading of the i=1 fiber row only. (a) The forces on the i=1 fiber separated into contributions from the squeezing flow and normal flow. (b) The forces on the i=2 to 4 fiber rows separated into the contributions from the squeezing and normal flows. The force due to the normal flow is greater than or equal to zero, while the force due to the squeezing flow is less than or equal to zero. From left to right are the i=2,3,4 force contribution.

Fig.5 Results for Lindt's problem of uniform top loading of the i=1 fiber row only, but with a reduced normal gap size, δ_o=0.5R. (a) The dimensionless fiber velocities V_i for i=1 to 3. Comparison with the larger normal gap results show that the free fall velocity for the consolidation front is reduced. (b) The forces on the i=1 fiber due to the squeezing and normal flows. (c) the forces on the i=2,3 fiber rows due to the squeezing and normal flows. From the left the forces on the i=2 fiber row are shown, with the normal force on the i=3 fiber increasing from zero, the squeeze force decreasing from zero, at t=5 seconds.

Fig. 6 Results for the uniform fiber tension on all i=n fiber rows. The force per unit length is T_c=0.005N/m, with μ=10kg/m-s, and $h_i(t=0)=\delta_o=R=10^{-5}$m. The i=n fiber row is considered stationary. (a) Half the dimensionless distance between adjacebt fiber rows, h_i^*, versus time, for i=7 to 11. Note that consolidation starts at the i=11 row and progresses upward. (b) Dimensionless fiber velocity, V_i^*, versus time, for i=7 to 11 fiber rows. Note that all of the fibers start with the free fall velocity given in equation (71) with T_1 replaced by T_1. (c) the forces on the fibers separated into contributions from the squeezing flow and normal flow. For the case of uniform tension on all the fibers rows, the rows which have consolidated are stationary, such that V_{i+1}=0. thus, the normal force on each fiber row decreases from one to zero, while the squeeze force increases from zero to one during the time each fiber is moving downward.

Fig. 7 Results for uniform tesion on all i=n fiber rows, but with a reduced normal gap size δ_o=0.5R. (a) Half the dimensionless distance between adjacent fiber rows, h_i^*, versus time for i=10,11. This case conforms more closely to the ideal free fall behavior. (b) The dimensionless fiber velocities, V_i^*, versus time for i=9 to 11. The initial free fall velocity is reduced due to the decrease in the normal gap size. (c) The forces on the i=11 fiber.

SYMBOL LIST

ρ	lc rho
U_c	cap U sub c
R	cap R
μ	lc mu
Re	Reynold's number
δ_o , δ_o^*	lc delta sub "oh", lc delta sub "oh" super *
$h_i(t)$, h_i, h_i^*	lc h sub i, sub "eye" super *
$V_i(t)$, V_i, V_i^*	cap "vee" of lc "tee" sub "eye", sub "eye", sub "eye" super *
U_i	cap "ewe" sub "eye"
η_i	lc eta sub "eye"
x_1, y_1, x_1^*, y_1^*	lc x and y, sub one, sub one super *
x_2, y_2, x_2^*, y_2^*	lc x and y, sub two, sub two super *
x, y, x^*, y^*	lc x and y, super *
∂	partial derivative
∇^2	Laplacian operator
∇	gradient operator
p_1, p_1^*	lc p, sub one, sub one super *
p_2, p_2^*	lc p, sub two, sub two super *
p_n, p_n^*	lc p, sub lc n, sub lc n super *
t, t^*	lc "tee", super *
Δt, Δt^*	cap delta lc "tee", super *
u_{x_1}, $u_{x_1}^*$	lc "ewe" sub lc x sub sub one

	as above with super *
u_{y_1}, $u^*_{y_1}$	lc "ewe" sub lc y sub sub one
	as above with super *
u_{x_2}, $u^*_{x_2}$	lc "ewe" sub lc x sub sub two
	as above with super *
u_{y_2}, $u^*_{y_2}$	lc "ewe" sub lc y sub sub two
	as above with super *
u_{x_n}, $u^*_{x_n}$	lc "ewe" sub lc x sub sub lc n
	as above with super *
u_{y_n}, $u^*_{y_n}$	lc "ewe" sub lc y sub sub lc n
	as above with super *
U_x	cap "ewe" sub lc x
V, P	cap "vee", cap "pee"
ε_i, ε_n	lc epsilon sub lc "eye", sub lc n
$f_2(x_2)$, f_2	lc f sub two of lc x sub two,
	lc f sub two
$f_n(y)$, f_n	lc f sub lcn of lc y, lc f sub lc n
Q_i	cap "cue" sub lc "eye"
q_i	lc "cue" sub lc "eye"
F^i_{ext}	cap F super lc "eye" sub lc "ext"
F^i_j	cap F super lc "eye" sub lc "jay"
σ^i_{jk}	lc sigma sub lc "jay" "kay"
	super lc "eye"
n	lc n (vector)
n_k	lc n sub lc"kay"

T_i, T_i^*	cap "tee" sub lc "eye", super *
θ	lc theta
Δp_n	cap delta lc "pee" sub lc n
T_c	cap "tee" sub lc "see"
t_c	lc "tee" sub lc "see"
ℓ	script lc "el"
W_r	cap "double ewe" sub lc r
$F^i_{x_{sq}}$	cap F super lc "eye" sub lc x sub sub lc "sq"
$F^i_{y_{sq}}$	cap F super lc "eye" sub lc y sub sub lc "sq"
$F^i_{y_{sq,bot}}$	cap F super lc "eye" sub lc y sub sub lc "sq,bot"
$F^i_{y_{sq,top}}$	cap F super lc "eye" sub lc y sub sub lc "sq,top"
$F^i_{x_n}$	cap F super lc "eye" sub lc x sub sub lc n
$F^i_{y_n}$	cap F super lc "eye" sub lc y sub sub lc n

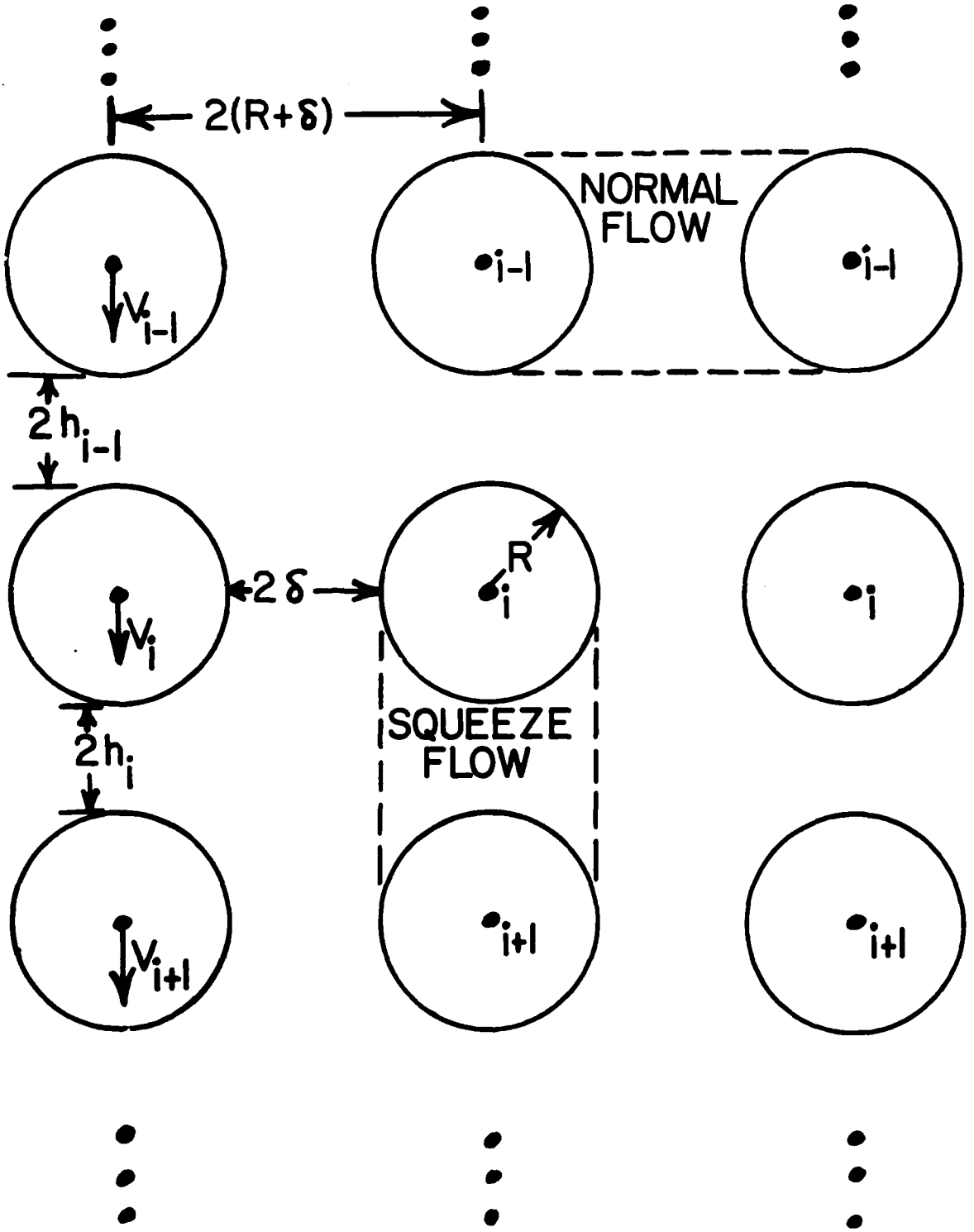
2(R+δ)
NORMAL
FLOW
i-1
i-1
V i-1
2h i-1
2δ
R
i
i
V i
2h i
SQUEEZE
FLOW
i+1
i+1
V i+1

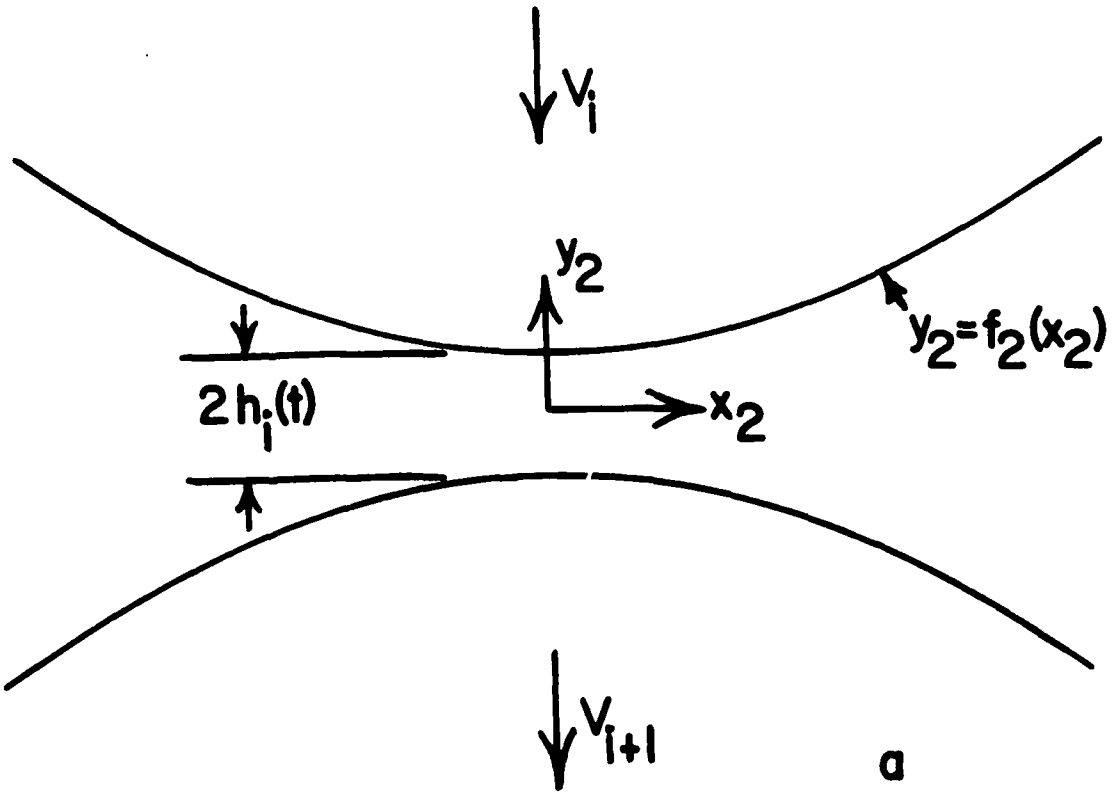

a

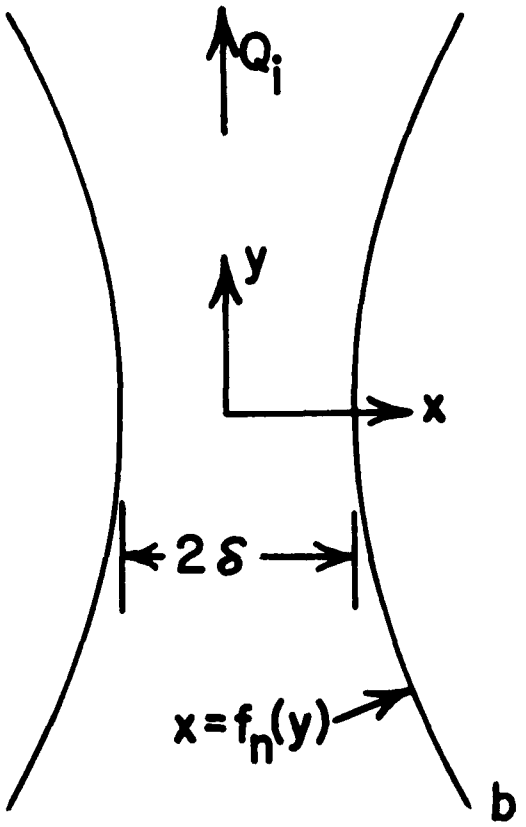
Q_i
y
x
2δ
$x = f_n(y)$
b

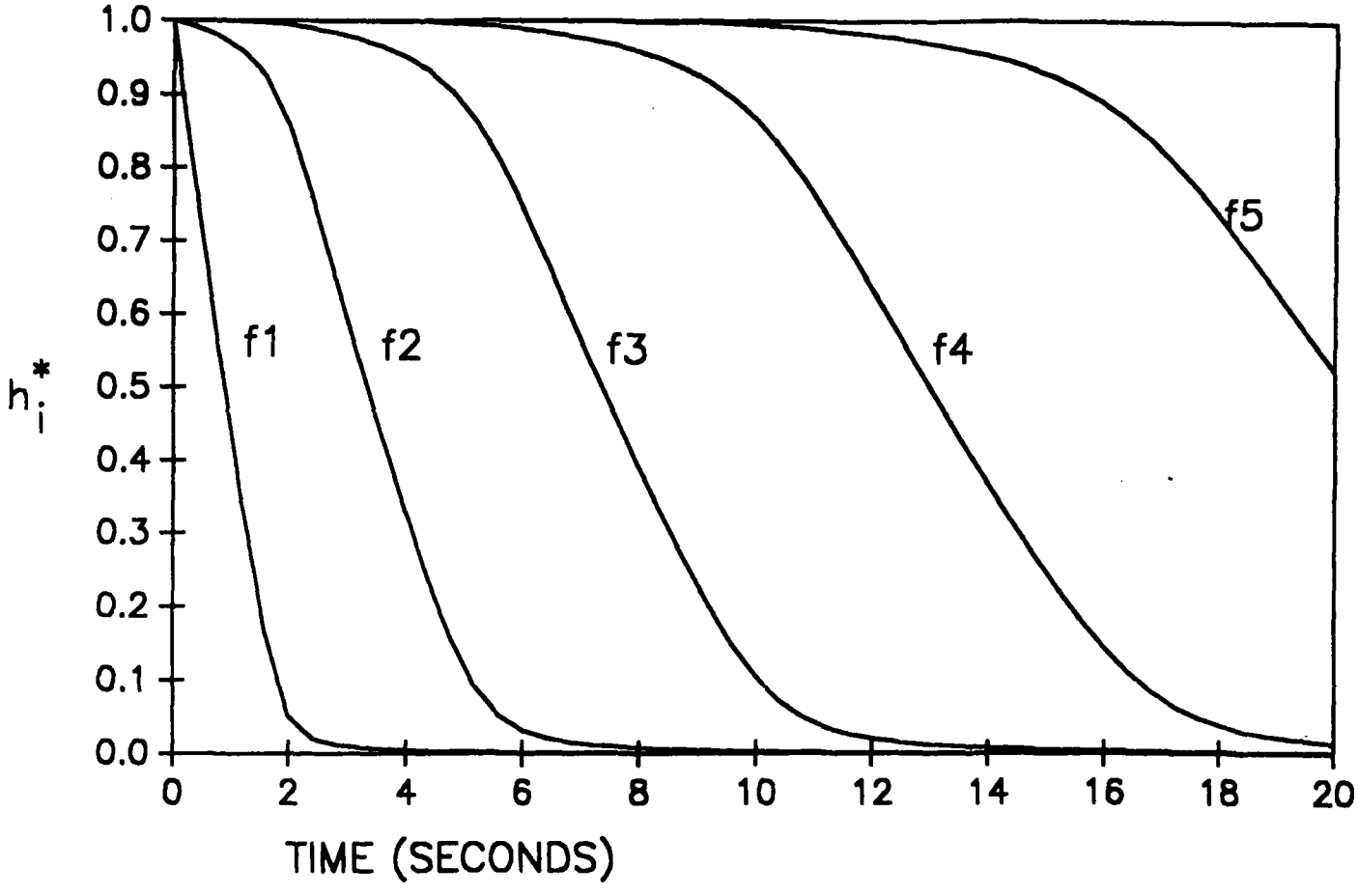

FIG 3(a) Hellmuth + Walker

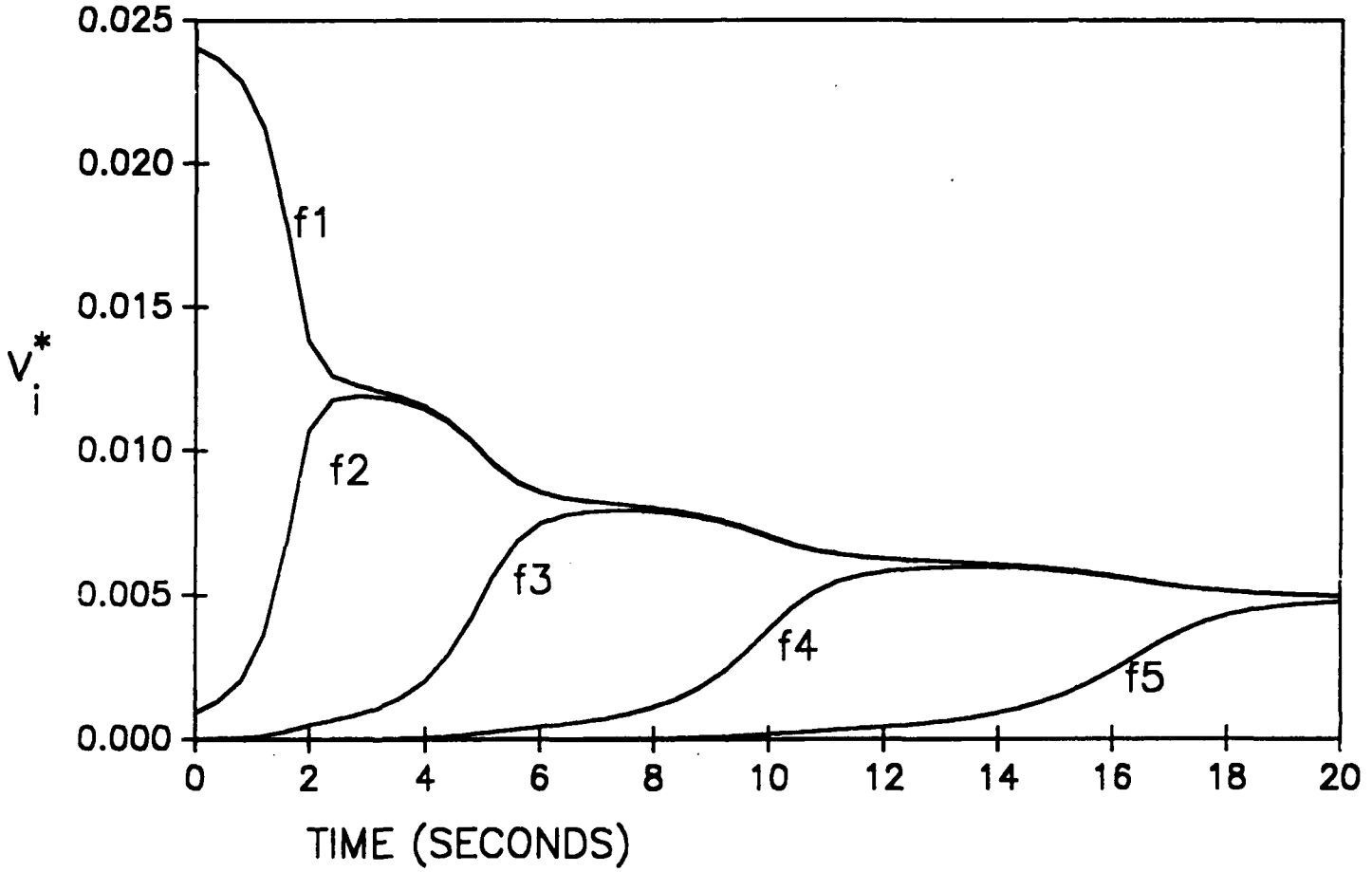

FIG 3(b) Hellmuq & Walker

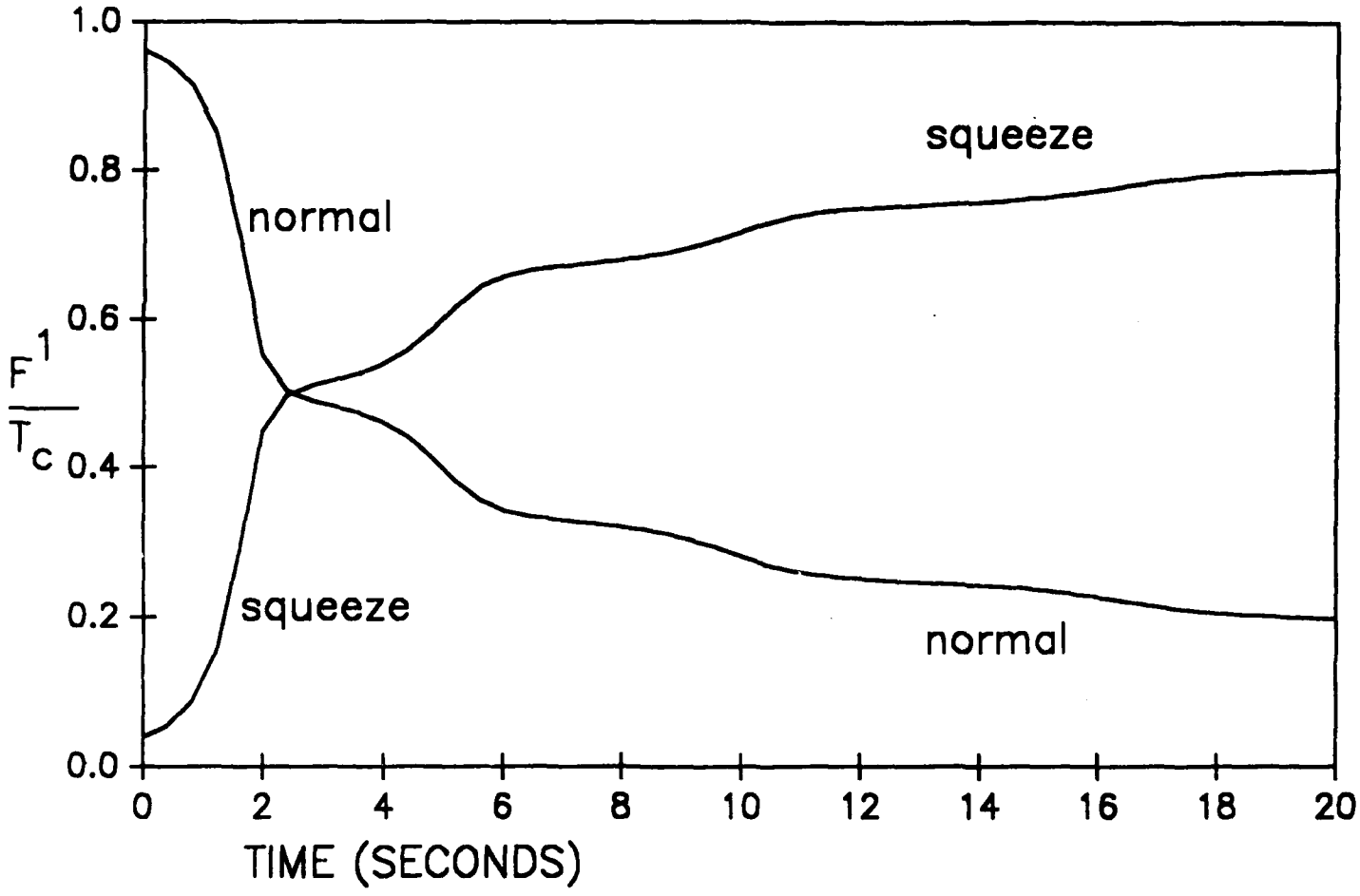

Fig 4(a) Hjellming + Walker

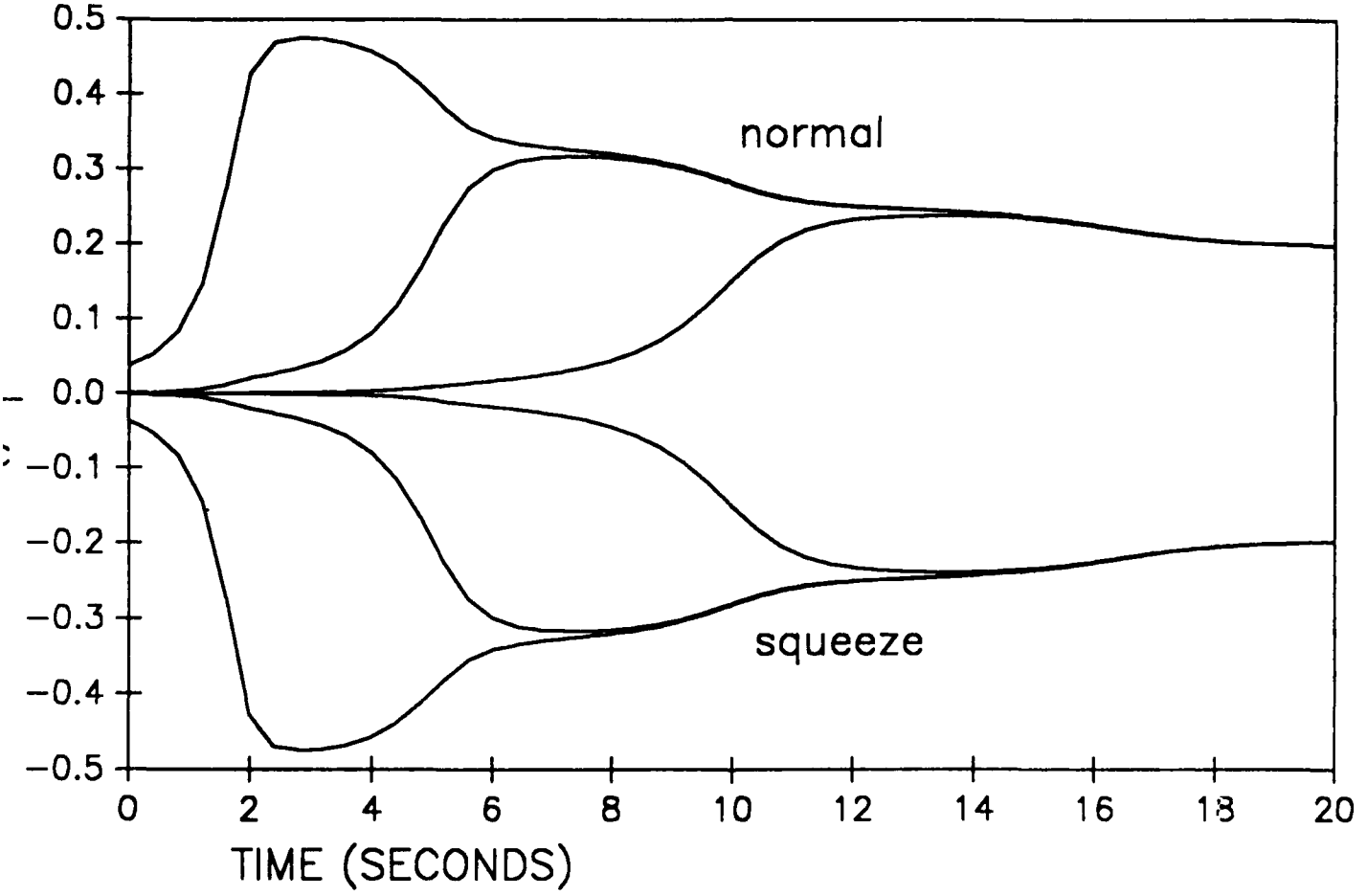

Fig 4(b) Hjellmug + Walker

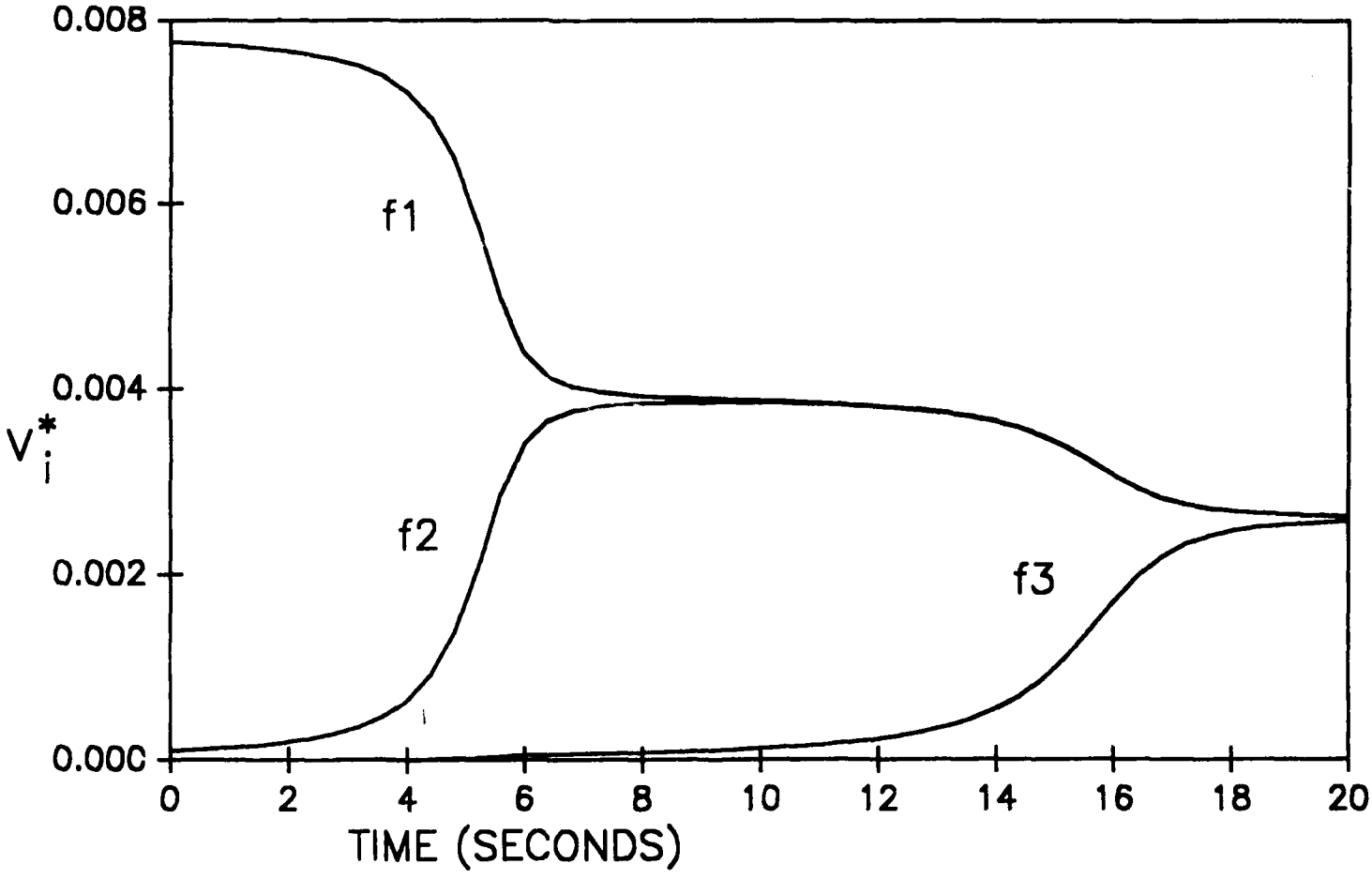

Figure 5(a) Hjellmyr + Walker

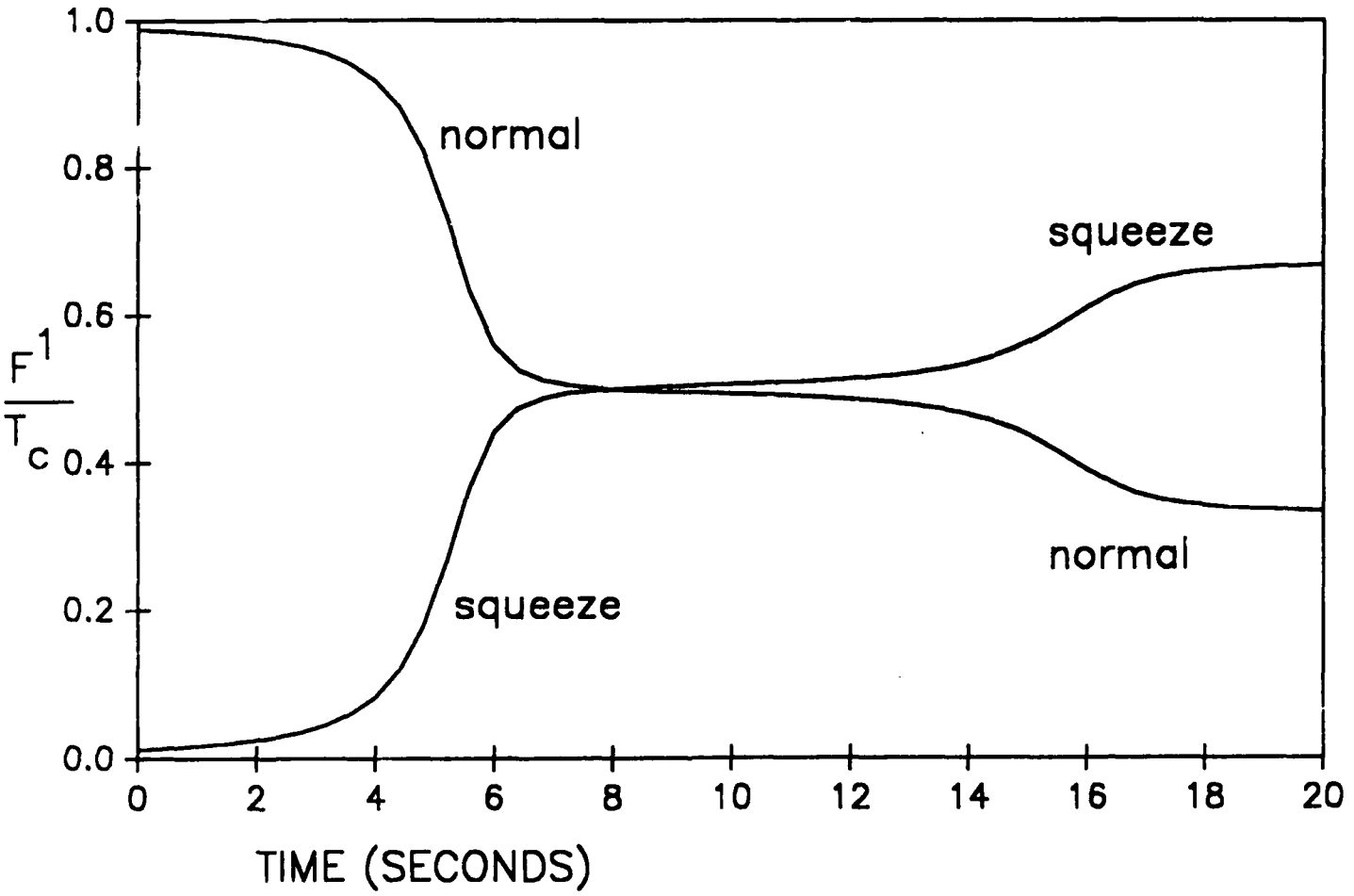

Figure 5(b) Hjellming + Walker

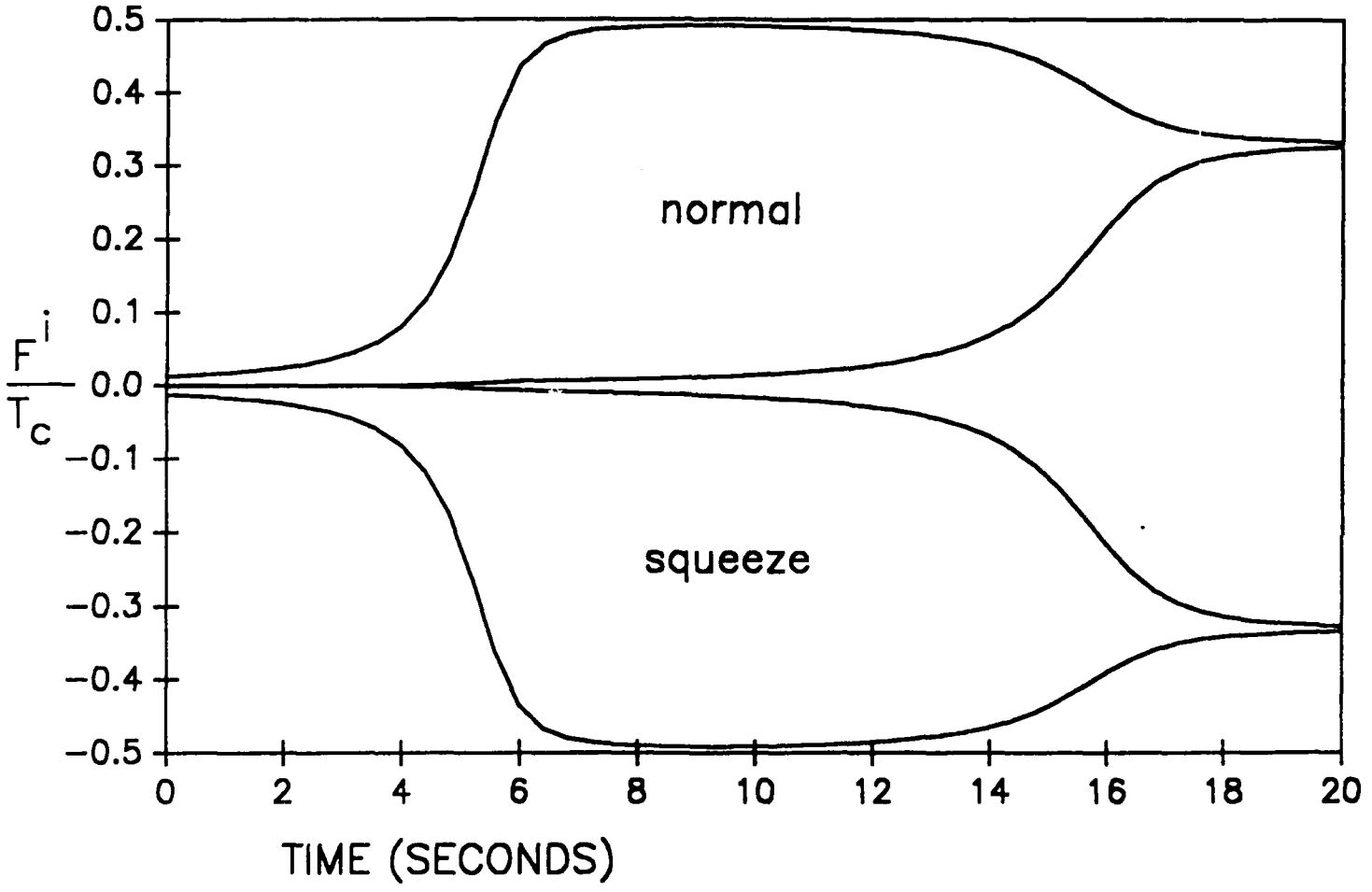

FIG 5(C) Hyllmuq & Walker

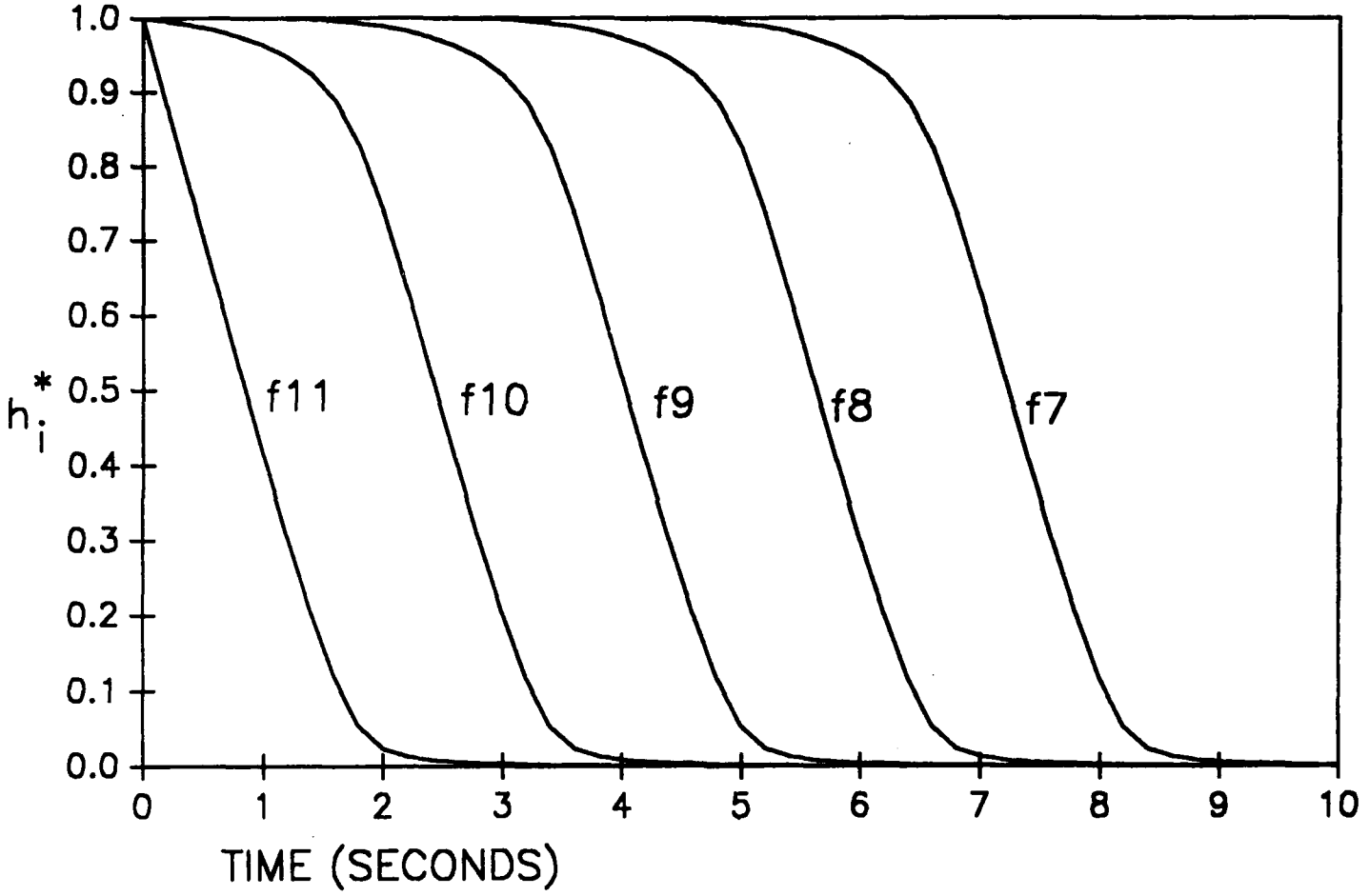

Fig. 6(a) Hjelmuq & Walker

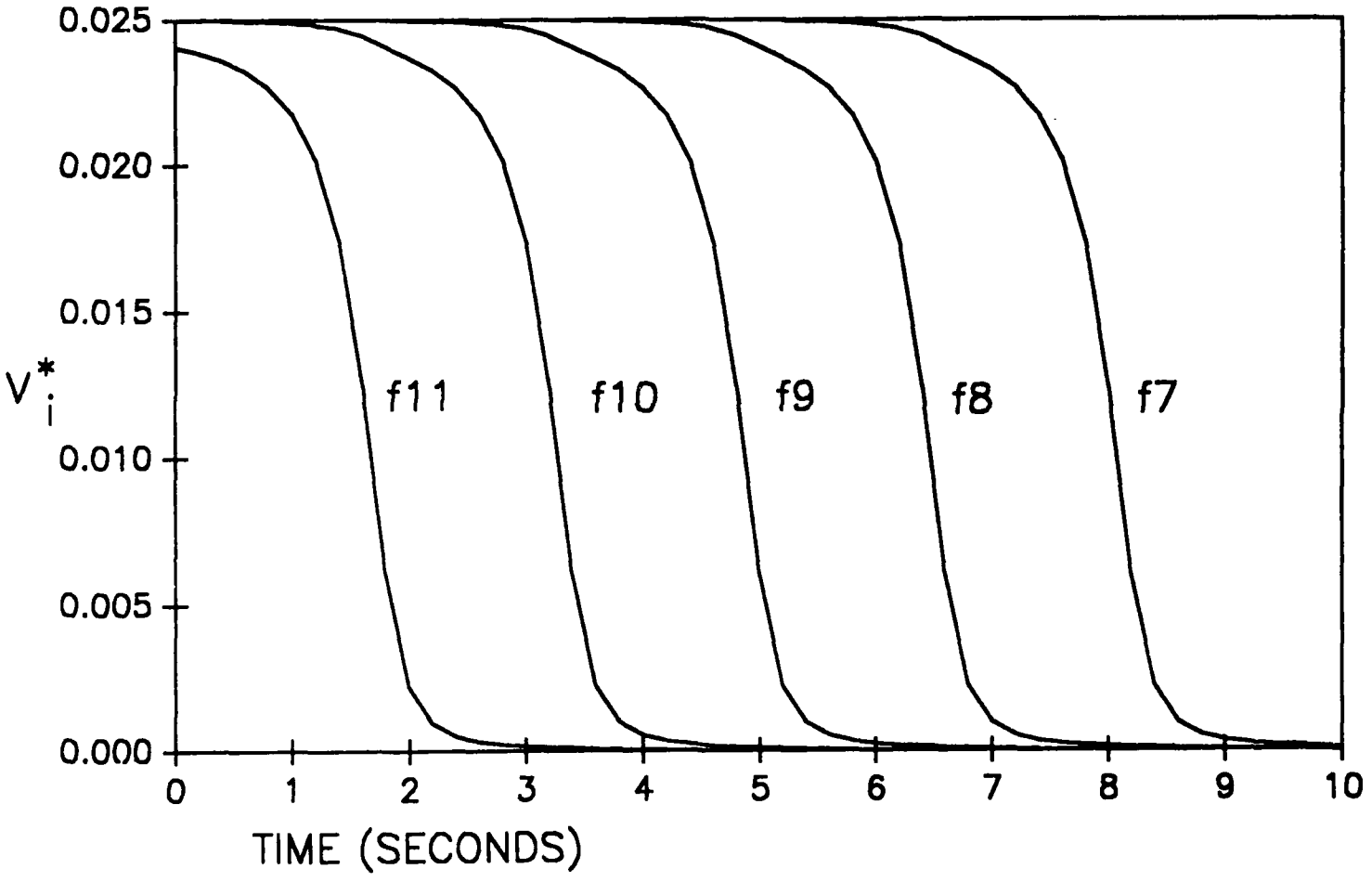

Fig 6(b) Hjellmung and Walker

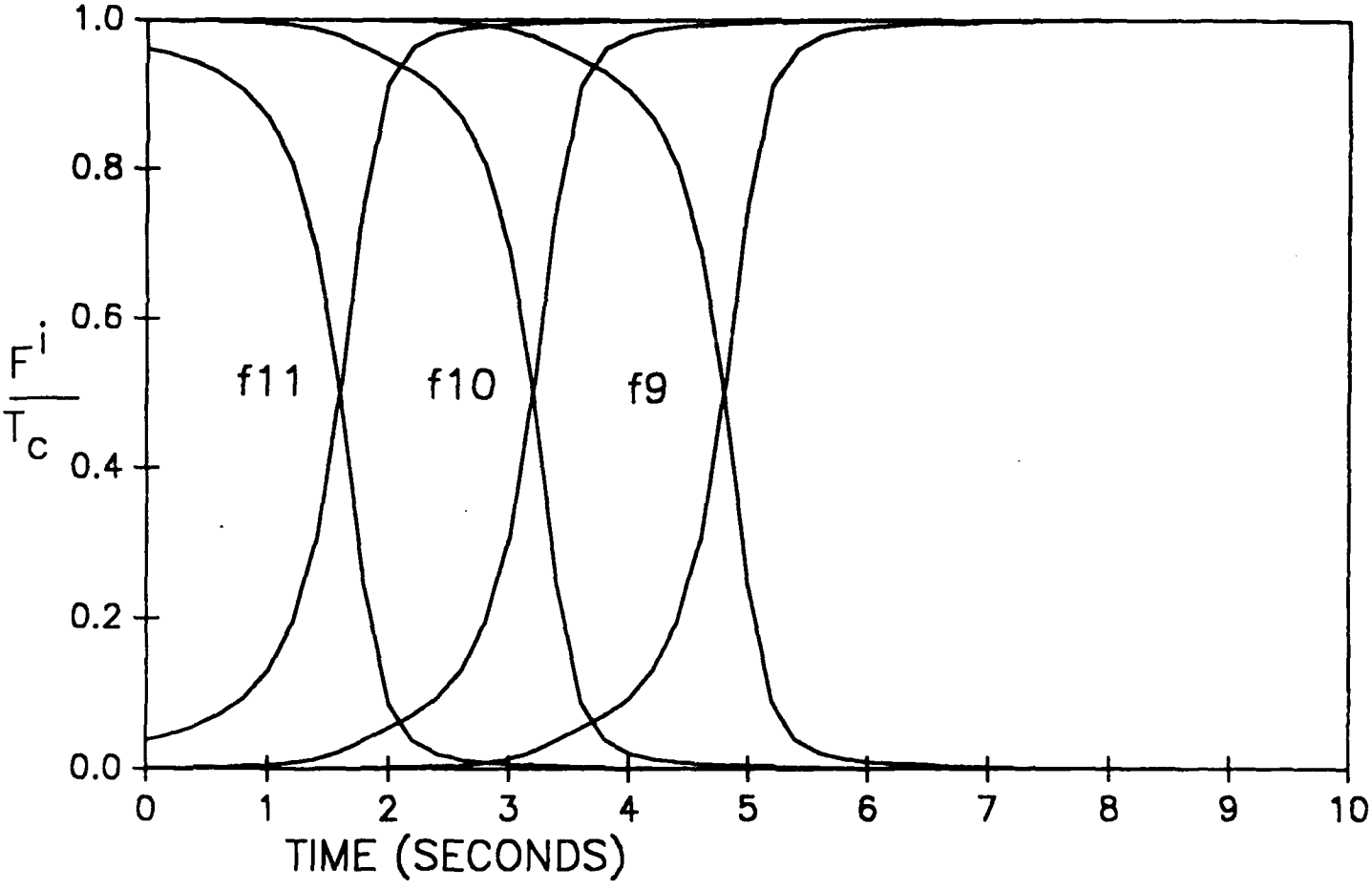

Fig 6(c) Hjellmuq + Walker

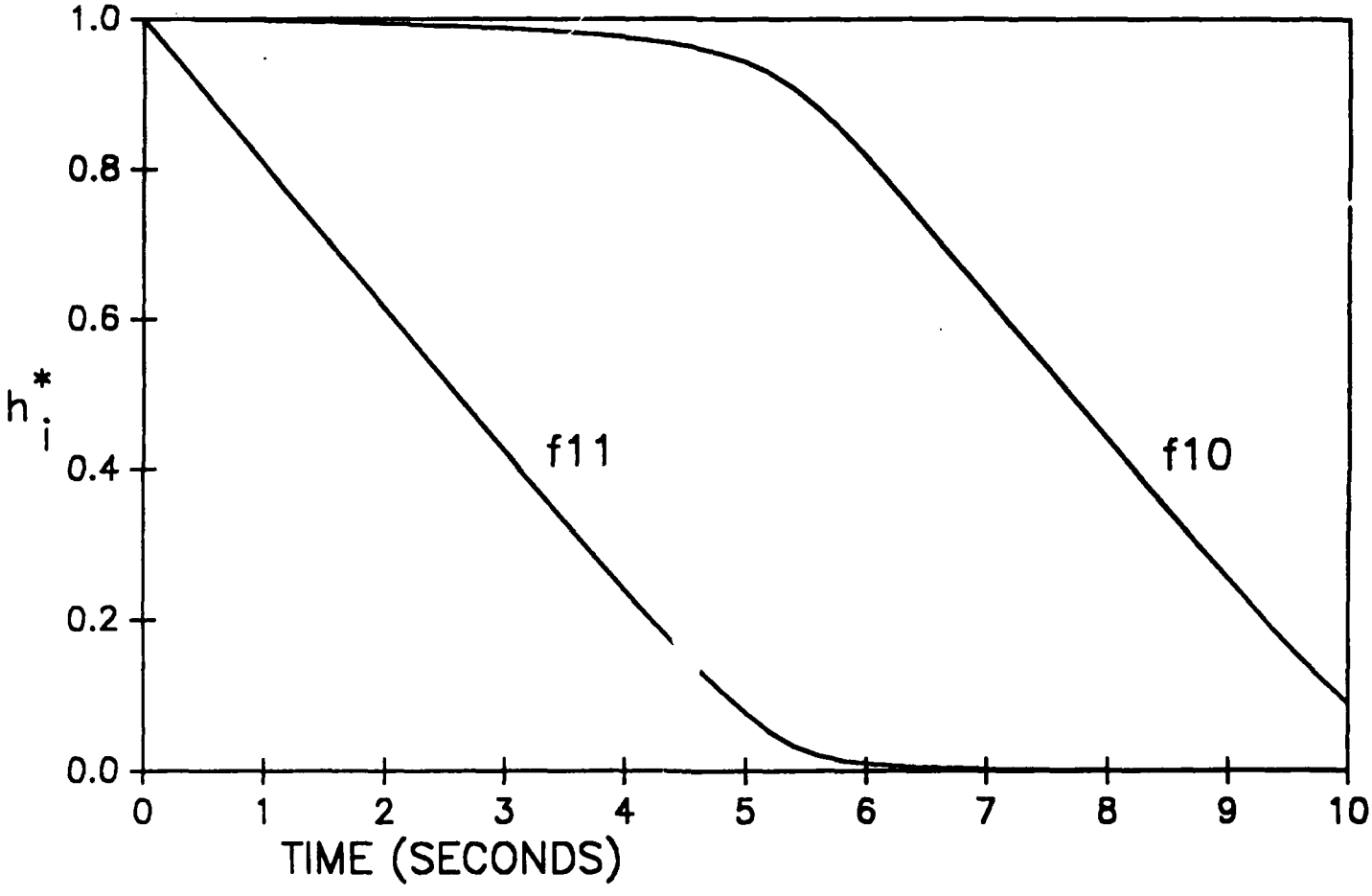

FIG 7(a) Hellmuth + Walker

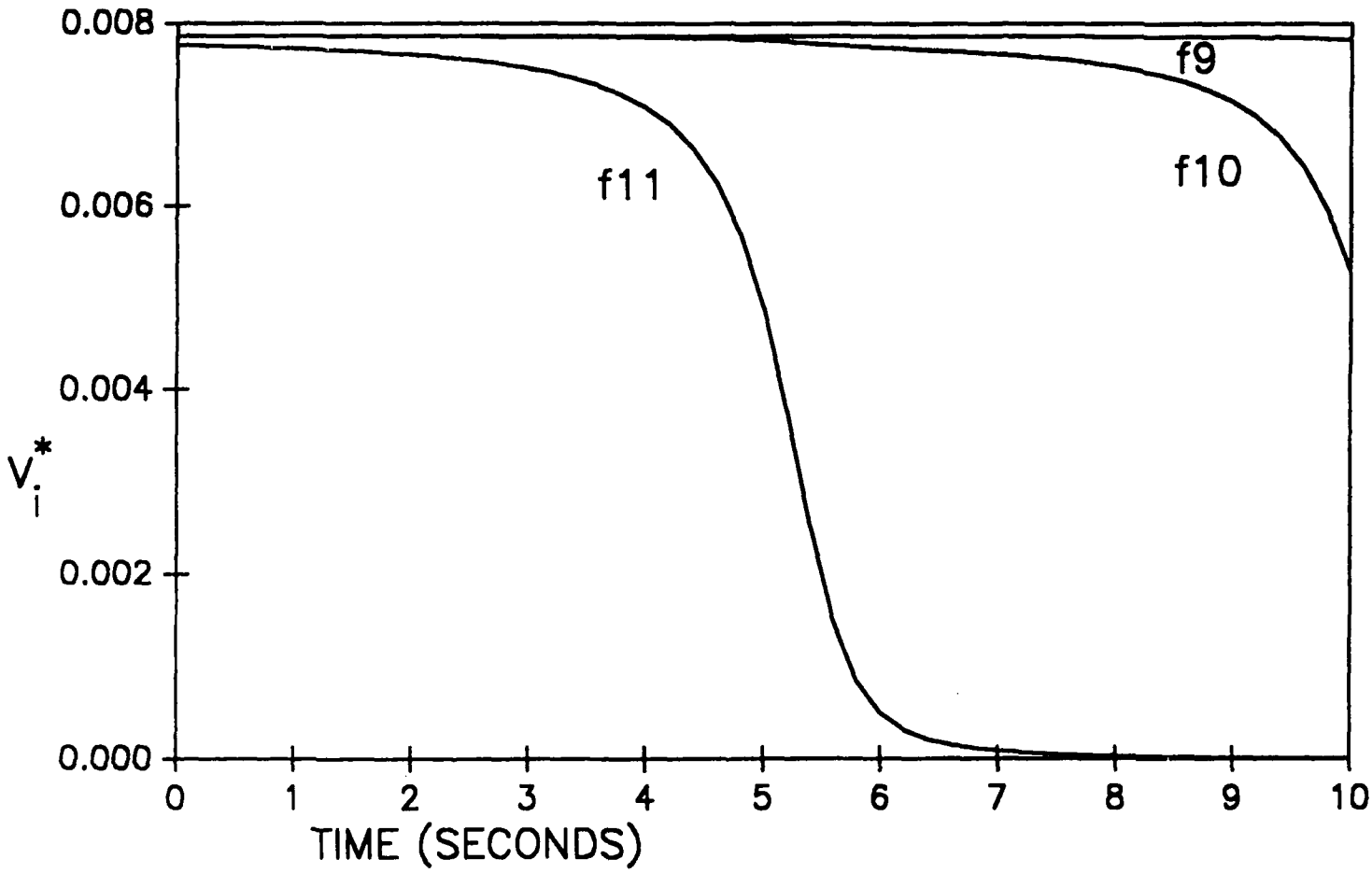

FIG 7(D) Hjellmung & Walker

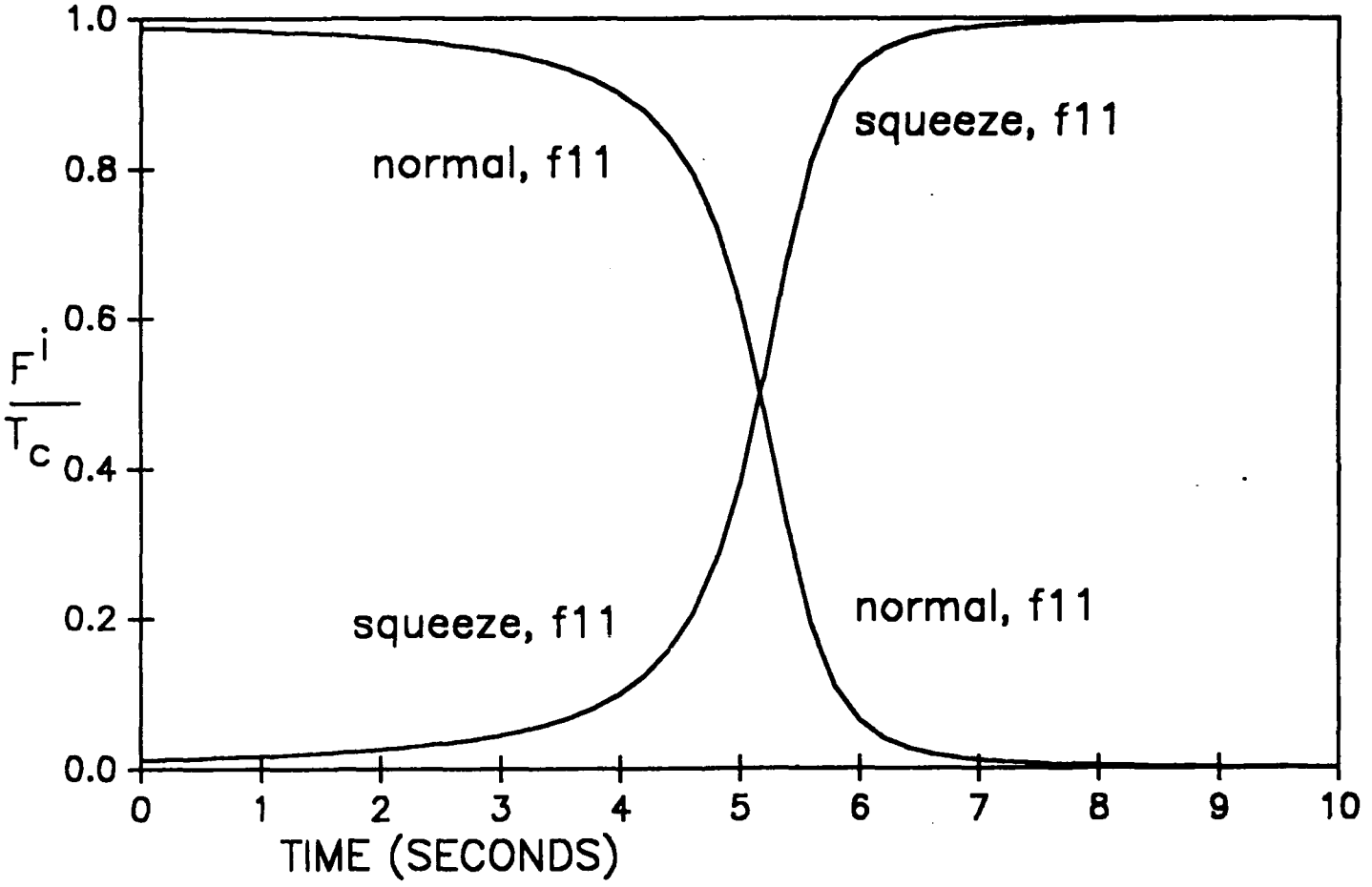

FIG 7(c) Hyellmuq + Walker